University of Alberta
Printing Department

THE UNIVERSITY OF ALBERTA

TRANSVERSE CURVATURE OF PLATES
UNDER LARGE DEFLECTIONS

A THESIS

SUBMITTED TO THE FACULTY OF GRADUATE STUDIES
IN PARTIAL FULFILMENT OF THE REQUIREMENTS FOR
THE DEGREE OF MASTER OF SCIENCE

DEPARTMENT OF MECHANICAL ENGINEERING

by

DONALD GRANT BELLOW, B.A.Sc.

EDMONTON, ALBERTA

April, 1960

UNIVERSITY OF ALBERTA
FACULTY OF GRADUATE STUDIES

The undersigned certify that they have read, and recommend to the Faculty of Graduate Studies for acceptance, a thesis entitled "Transverse Curvature of Plates Under Large Deflections" submitted by Donald Grant Bellow in partial fulfilment of the requirements for the degree of Master of Science.

A B S T R A C T

A new experimental approach to observing the transverse curvature of a plate when subjected to large deflections is presented. Through the use of "SR-4" strain gauges placed in the transverse direction on a plate it is shown that the transverse curvature is dependent on a dimensionless ratio $\frac{b^2}{Rd}$. In this thesis some discrepancies arise between the experimental evidence and the available theory. It is suggested that these discrepancies may be due to the plates being distorted previously to testing. A possible method of determining the bounds of Saint-Venant's Principle is also shown.

ACKNOWLEDGEMENTS

The author sincerely thanks Professors G. Ford and J.S. Kennedy for all the assistance and encouragement given him in the preparation of this thesis.

Thanks are also due to the Mechanical Engineering Department of the University of Alberta which provided the best material and equipment available for the experimental work.

TABLE OF CONTENTS

LIST OF FIGURES

NOTATION

b = Transverse width of beam or plate (in)

d = Thickness of beam or plate (in)

e = Strain $\left(\frac{in}{in}\right)$

E = Young's modulus $\left(\frac{lbs}{in^2}\right)$

I = Moment of inertia of a cross-section (in^4)

M = Bending moment in the beam (in-lbs)

R = Radius of curvature (in)

ν = Poisson's ratio

σ = Stress $\left(\frac{lbs}{in^2}\right)$

Chapter 1 - OBJECTIVES

The experimental work in this thesis was undertaken with three main objectives in mind;

1. To show that the ratio $\frac{b^2}{Rd}$ is a true physical parameter.

2. To observe the edge effect as indicated by Ashwell, and Fung and Wittrick.

3. To establish if strain gauges can be used to obtain a satisfactory analysis of anticlastic curvature.

Chapter 2 - INTRODUCTION

When a beam, whose width b is of the order of its thickness d, is bent to a radius R, the strain in the longitudinal direction a distance y from the neutral axis is given by $e_z = \frac{y}{R}$. Since there is no stress in the transverse direction (i.e., the beam is free to distort) then the transverse strain is $e_x = -\nu e_z$, where ν is Poisson's ratio. This is an anticlastic surface, an example of which is shown in Figure 1. This result was shown as early as 1864 by Saint-Venant.

For simple beam theory it can be shown that

$$\frac{1}{R} = \frac{M}{EI} \doteq \frac{-d^2y}{dx^2} \quad \ldots\ldots\ldots\ldots\ldots\ldots \quad 1$$

where, M is the applied moment producing the curvature $\frac{1}{R}$.

E is the modulus of elasticity for the material.

I is the moment of inertia of the undistorted cross-section parallel to the axis of bending.

When a flat plate, with two opposite edges simply supported and the other two free, is bent by moments applied along the supported edges, and the width parallel to the supports is infinite, distortion in the transverse direction is prevented. Hence, there is no strain in the transverse direction and the transverse curvature is zero.

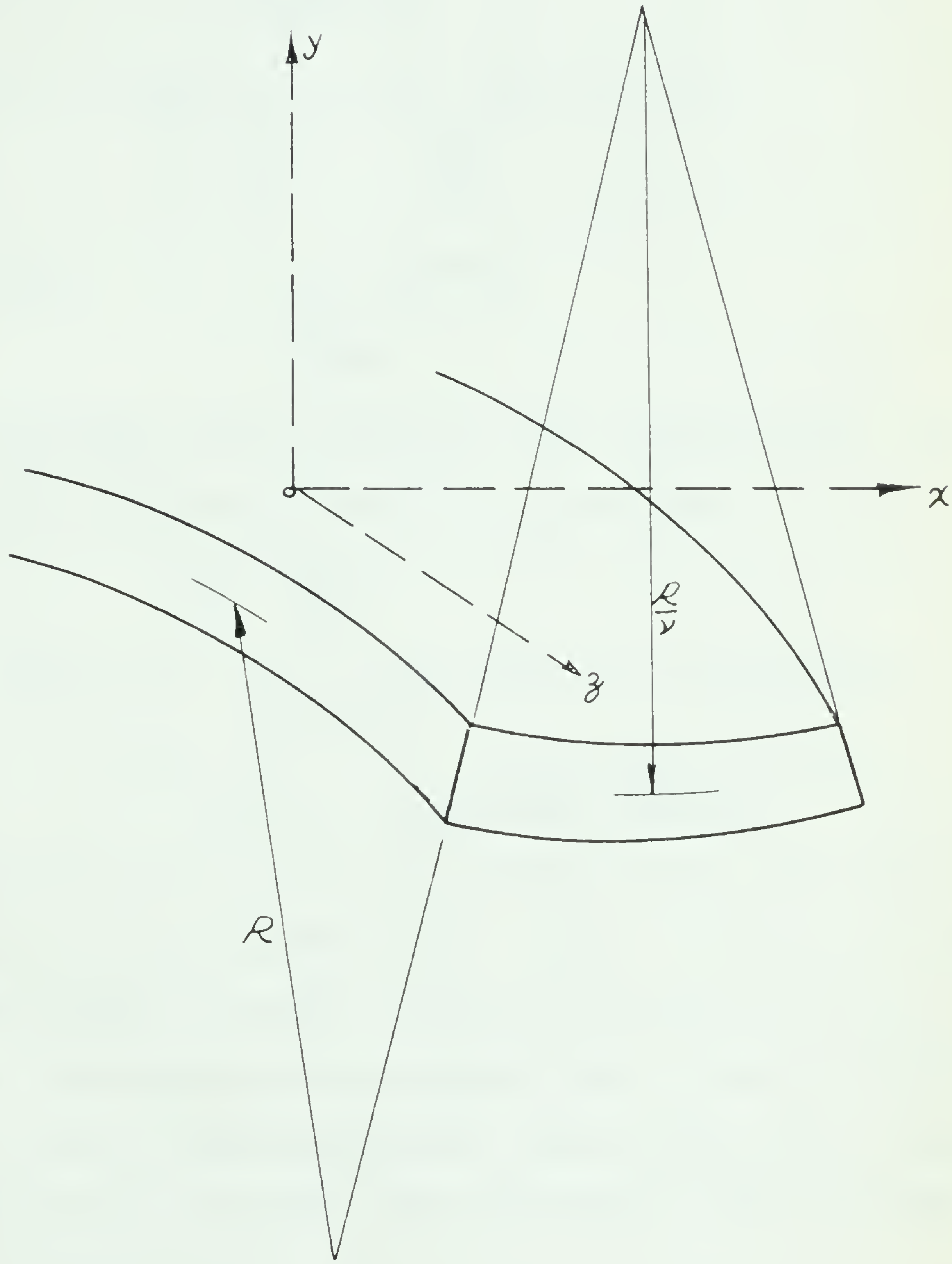

FIGURE 1. BEAM BENT WITH AN ANTICLASTIC CURVATURE

therefore,

$$\sigma_x = \nu \sigma_z$$

$$\sigma_z = \frac{e_z E}{(1-\nu^2)}$$

thus, $$M = \frac{E}{(1-\nu^2)R} \frac{d^3}{12}$$

for a longitudinal strip one unit wide,

$$\frac{1}{R} = \frac{M}{E'I} \doteq -\frac{d^2y}{dx^2} \quad \ldots\ldots\ldots\ldots\ldots \; 2$$

where E' = plate modulus

$$= \frac{E}{(1-\nu^2)}$$

Equations 1 and 2 represent two extreme cases. For the general case, the curvature is given by;

$$\frac{1}{R} = \frac{M}{E\phi I}$$

where $\phi = 1$ for a beam subject to anticlastic curvature

$\phi = \frac{1}{(1-\nu^2)}$ for a plate bent to a true cylindrical surface.

Searle (1)* studied the problem of the transition from beam action to plate action. Case (2) showed, in much the same manner as Searle, that if a beam was bent to a radius R there developed resultant radial forces parallel to the plane of bending which, if large enough, would reduce the transverse curvature. The analysis of Case has been shown in Appendix A.

---

* Numbers in parentheses refer to references in the bibliography.

Searle and Case argued that in order for a beam to have an anticlastic curvature equal to $\frac{-\nu}{R}$ the ratio $\frac{b^2}{Rd}$ must be much less than 12.

For a plate Searle and Case estimated that the resultant radial forces would neutralize the anticlastic curvature at the center of the transverse section for $\frac{b^2}{Rd}$ greater than 6. They allowed that there would be a slight curvature at the edges. Figure 2 shows the type of plate action expected by Searle and Case.

Further to the above, Case postulated that the transition from beam action to plate action would not be gradual but would occur suddenly. He agreed with Searle in that the ratio $\frac{b^2}{Rd}$ determined the mode of transverse curvature.

Ashwell (3) largely followed the work of Searle and Case. To analyze the slight curvature at the edges (i.e., the edge effect) Ashwell employed a fourth order differential equation (it was first developed by Lamb in 1891) which included the dimensionless ratio $\frac{b^2}{Rd}$. The manner in which Ashwell derives this equation is given below. For a longitudinal strip of a plate bent to a radius R (see Figure 3) there develops, due to the anticlastic curvature, longitudinal forces F which have a resultant in the radial direction equivalent to $F_r = Fd\theta$ (see Appendix A)

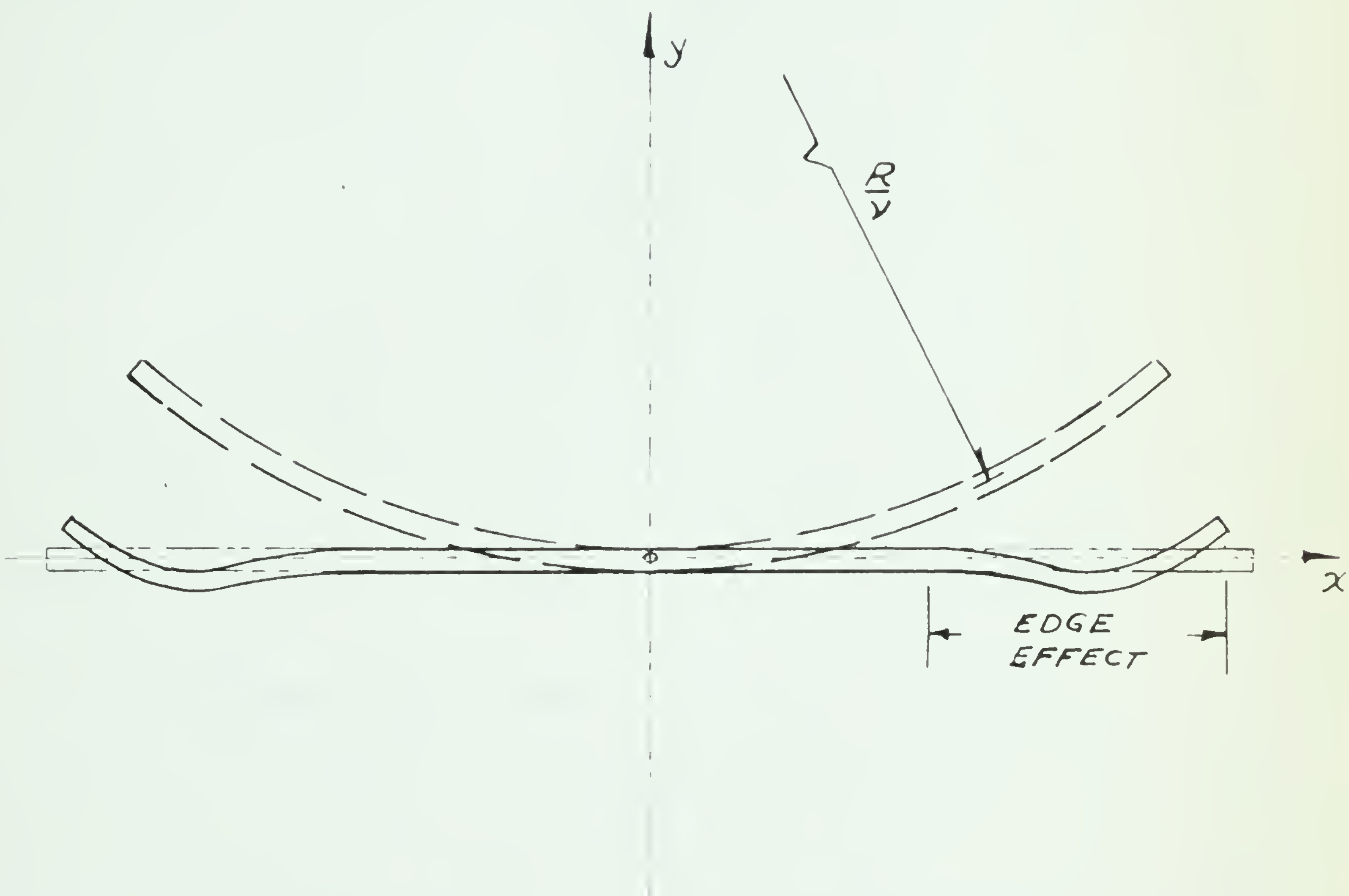

FIGURE 2. PLATE ACTION WHEN RADIAL FORCES ARE SUFFICIENT TO NEUTRALIZE ANTICLASTIC CURVATURE

LONGITUDINAL SECTION

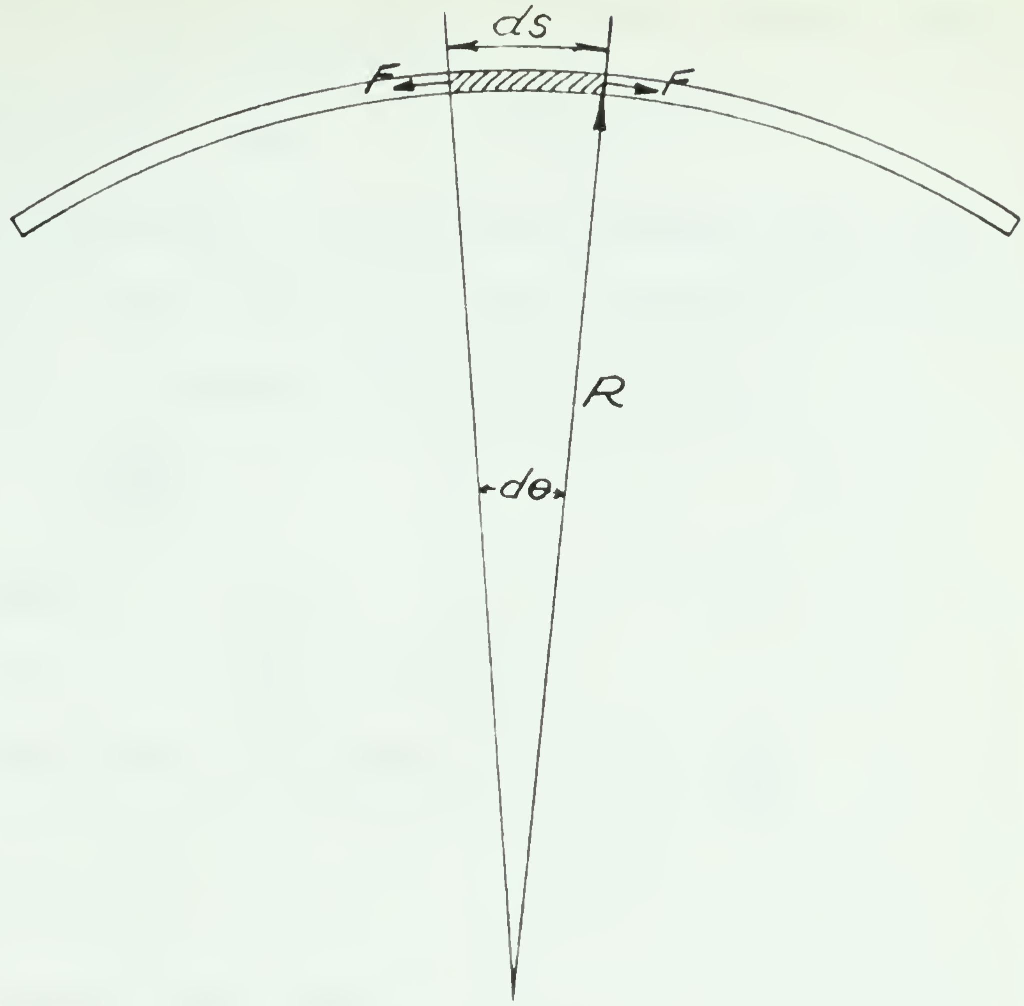

TRANSVERSE SECTION

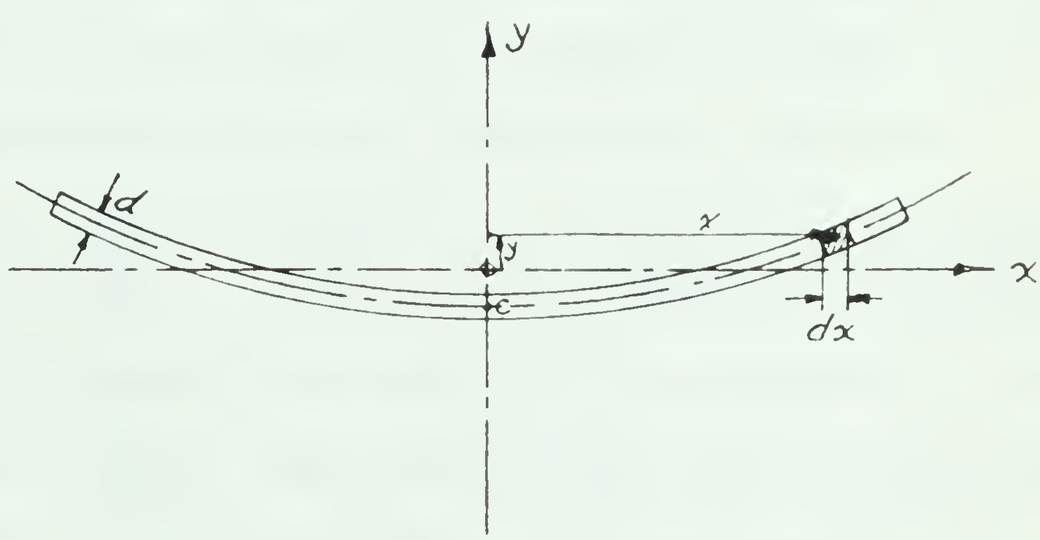

FIGURE 3. FORCES ON A PLATE

where F is longitudinal force acting along the element ds.

and, $ds = Rd\theta$

This resultant radial force acting over the length ds and over a unit length in the transverse direction is equivalent to a pressure and is given by

$$\frac{Fd\theta}{ds.1}$$

since $F = \sigma\, dA$

or, $F = \frac{yE}{R}\, d\ (1)$

therefore, $\text{Pressure} = \frac{yEd}{R} \cdot \frac{d\theta}{ds}$

$$= \frac{yEd}{R^2}$$

The transverse strip is subject to a non-uniform distributed load equal to $\frac{yEd}{R^2}$. This load is proportional to y the distance from the middle surface to the x - axis.

It is known that the deflection of a beam, under the action of a non-uniformly distributed load, can be obtained from the following differential equation;

$$\frac{d^4y}{dx^4} + \frac{Ky}{EI} = 0$$ (i.e., equation for a beam on an elastic foundation)

Ashwell argues that the E in this equation is the Plate E' (i.e., $\frac{E}{1-\nu^2}$). The assumptions that he made are that $(\frac{dy}{dx})$ is small and the distortion of the transverse strip is not large.

Therefore, from the above

$$\frac{d^4y}{dx^4} + \frac{yEd}{E'R^2I} = 0$$

$$\text{and,} \quad I = \frac{1\,(d)^3}{12}$$

$$\text{therefore,} \quad \frac{d^4y}{dx^4} + \frac{12\,(1-\nu^2)}{R^2d^2}\,y = 0 \quad \ldots\ldots\ 3$$

Solving equation 3 Ashwell found that when y versus x was plotted, $\frac{b^2}{Rd}$ predicted the mode of distortion. Using the solution he plotted the edge effect and observed how it varied for different $\frac{b^2}{Rd}$ values. From these curves Ashwell concluded that for $\frac{b^2}{Rd} > 100$ the transverse curvature is confined to the edges of the plate. He further estimated, for $\frac{b^2}{Rd}$ very large (i.e., greater than 400) that the deviation in the transverse deflection at the edges was a constant value equivalent to 10 percent of the plate thickness. In the derivation Ashwell assumed that the slope $\frac{dy}{dx}$ was very small and that any shear stress in the transverse section was negligible.

Fung and Wittrick (4) analyzed the same problem and their results show the same edge-effect for large $\frac{b^2}{Rd}$ values.

Ashwell and Greenwood (5) conducted experiments to test the above theories. They found, however, under the most carefully planned test that the experimental work did not agree very closely with the theoretical calculations, even for $\frac{b^2}{Rd} < 10$. They attributed this discrepancy to the fact that if the plate had an initially small curvature, it markedly affected the final transverse curvature. No matter how much care was taken in handling the plate they found it was impossible to

avoid some distortion. They expressed disappointment in their experimental work and they emphasized that it was a very difficult experiment to perform.

Hall, Pinkney and Tullock (6,7) reported that the effective elastic modulus E found in tests conducted on swept-back wings did not coincide with the plate E as expected. This phenomenon which they observed is undoubtedly related to the problem of transverse curvature discussed by Searle, Case and Ashwell.

Largely as a result of Hall's observations and his subsequent communications to Dr. Ford, it was decided to study the problem experimentally at the University of Alberta.

Chapter 3 - EXPERIMENTAL

A. General

To observe the mode of anticlastic behaviour in an initially flat plate it was thought that deflections measured by accurate dial gauges would yield the best results. This is the method which is described by Ashwell and Greenwood (5). However, in an earlier work Ashwell and Greenwood (8) point out the disadvantages of using a dial gauge on a thin plate. The main objection was that the spring force of the dial gauge itself imparted an additional significant deflection to the plate.

A dial gauge was used to measure plate deflections at the University of Alberta, and the same objections were noted. Removal of the spring and thus, the force exerted on the plate, reduced the local deflection but because of a reduced contact pressure of the dial gauge, it was found that repeated readings were inconsistent. In their experimental work, Ashwell and Greenwood describe a method of determining the anticlastic curvature by measuring the angle changes of a light beam reflected at a point on the plate surface. To do this they used an "Angle Dekkor" which is a type of optical autocollimator. Since no autocollimator was available at the University of Alberta, it was decided that the anticlastic curvature could be observed by the use "SR-4" bonded filament strain gauges placed back to back

on top and bottom of the plate in the transverse direction.

It was decided that the plate material be aluminum of high tensile properties in order to obtain large deflections without any yielding. The aluminum chosen was "Alcan, Alclad 75 ST-6". In determining the correct plate size two factors became apparent. First, it was desirable to have a large $\frac{b^2}{Rd}$ ratio. This necessitated that the plates be wide and thin. However, if the plates were too wide and too thin there would be a possibly of warping due to machining and handling. Secondly, the length of the plate was important. The plate had to be long enough in order that the mid-line in the transverse direction would not be influenced by any secondary effects of the supports or method of loading.

Saint-Venant's Principle states that at some finite distance away from a disturbing force the stresses are uniform and unaffected by the manner in which the disturbing force is applied. The meaning of a "finite distance away" seems rather obscure. Various references were consulted but all were vague about the "distance away". The best definition probably comes from Den Hartog (9) who says " .... the 'principle' is not an exact mathematical theorem, but rather a practical or common-sense proposition ...."

With this principle in mind the distance between supports was chosen as 3 feet with an overall plate length of 6 feet.

As one of the objectives of this work was to show that the ratio $\frac{b^2}{Rd}$ was a true physical parameter, it was decided to test plates of varying width and thickness. The final choice of the plate sizes, which was somewhat arbitrary, are as follows;

1/8 x 10 x 72 inch

1/8 x 18 x 72 "

1/8 x 28 x 72 "

1/8 x 38 x 72 "

1/16 x 38 x 72 "

3/16 x 38 x 72 "

1/4 x 38 x 72 "

With these plate sizes it was possible to test each plate so that the $\frac{b^2}{Rd}$ values thus obtained overlapped those obtained using the other plates.

The "Alclad 75 ST-6" aluminum sheets were purchased in sizes 12 feet by 4 feet. This meant that the sheets had to be cut to size. Originally, it was planned to have a sheet metal shop shear the plates. However, it was thought the shearing action would impart strains into the metal. Cutting the sheets by means of an oxy-acetylene torch was also considered but because of the high thermal conductivity of aluminum, and the fact that "Alclad 75 ST-6" is a heat treated metal, it was believed that the heat from the torch would anneal the plates and alter the mechanical properties,

causing distortion. It was finally decided that the least harm to the metal could be obtained by sawing. Because of the large sheet size it was impossible to use a band saw or any other heavy duty machine. Sawing was accomplished by the use of an electrical hand-held jig-saw. This method, although tedious and laborious, resulted in a clean cut with a minimum of plate distortion.

Figures 4 and 5 and Appendix B show the general layout of the test apparatus. The plates were simply supported with the load applied outside the supports. This loading subjected the plate to pure bending. The fixed and the roller support each had a contact radius of 3/8 inch. As the plate deformed the roller moved towards the fixed support decreasing the distance between supports by as much as 1/8 inch for the largest deflections. This was neglected in calculations.

For all but the 1/16 inch thick plate, the load was applied in the same manner. As shown in Figure 6, the load was applied by placing weights on a hanger which acted on a thin angle piece bolted to the plate. For the 1/16 inch thick plate the weights were placed directly on the metal surface as shown in Figure 7.

A single dial gauge, with the return spring removed, was placed so that it measured deflections at the geometric center of the plate. These dial gauge readings were not

FIGURE 4. STRAIN INDICATOR AND SWITCHING BOX

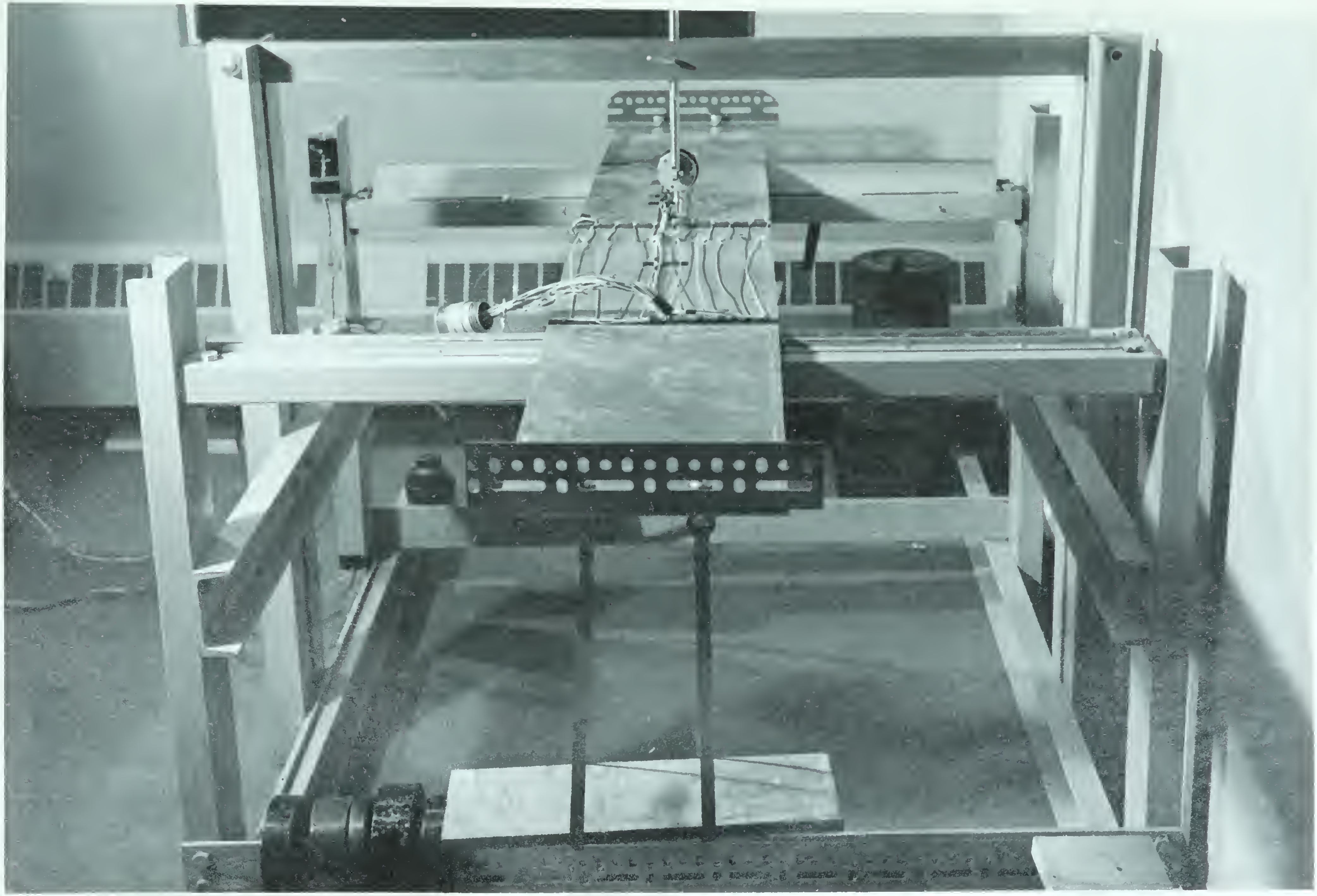

FIGURE 5. GENERAL VIEW OF TEST FIXTURE

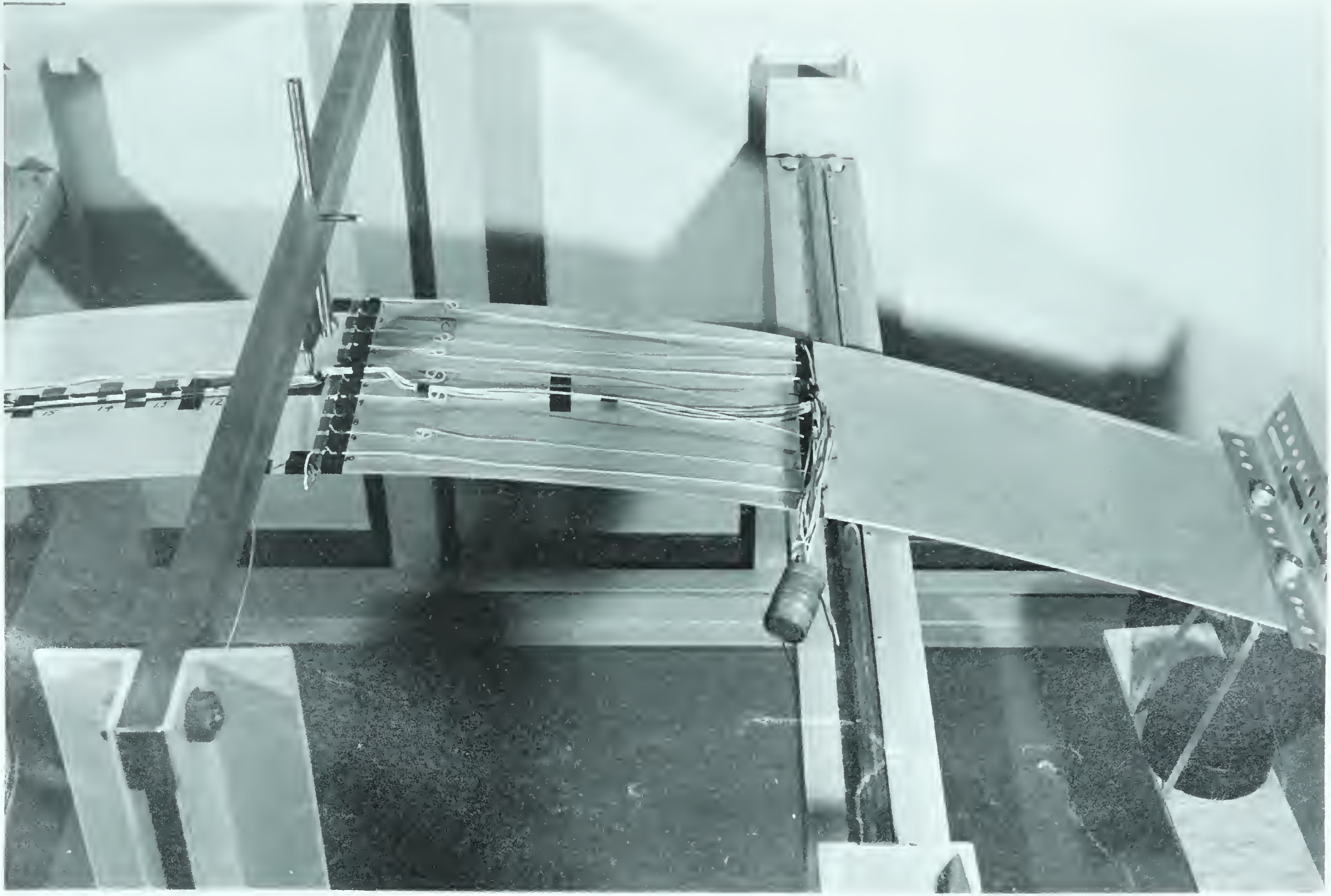

FIGURE 6. LARGE DEFLECTION OF PLATE SHOWING METHOD OF LOADING

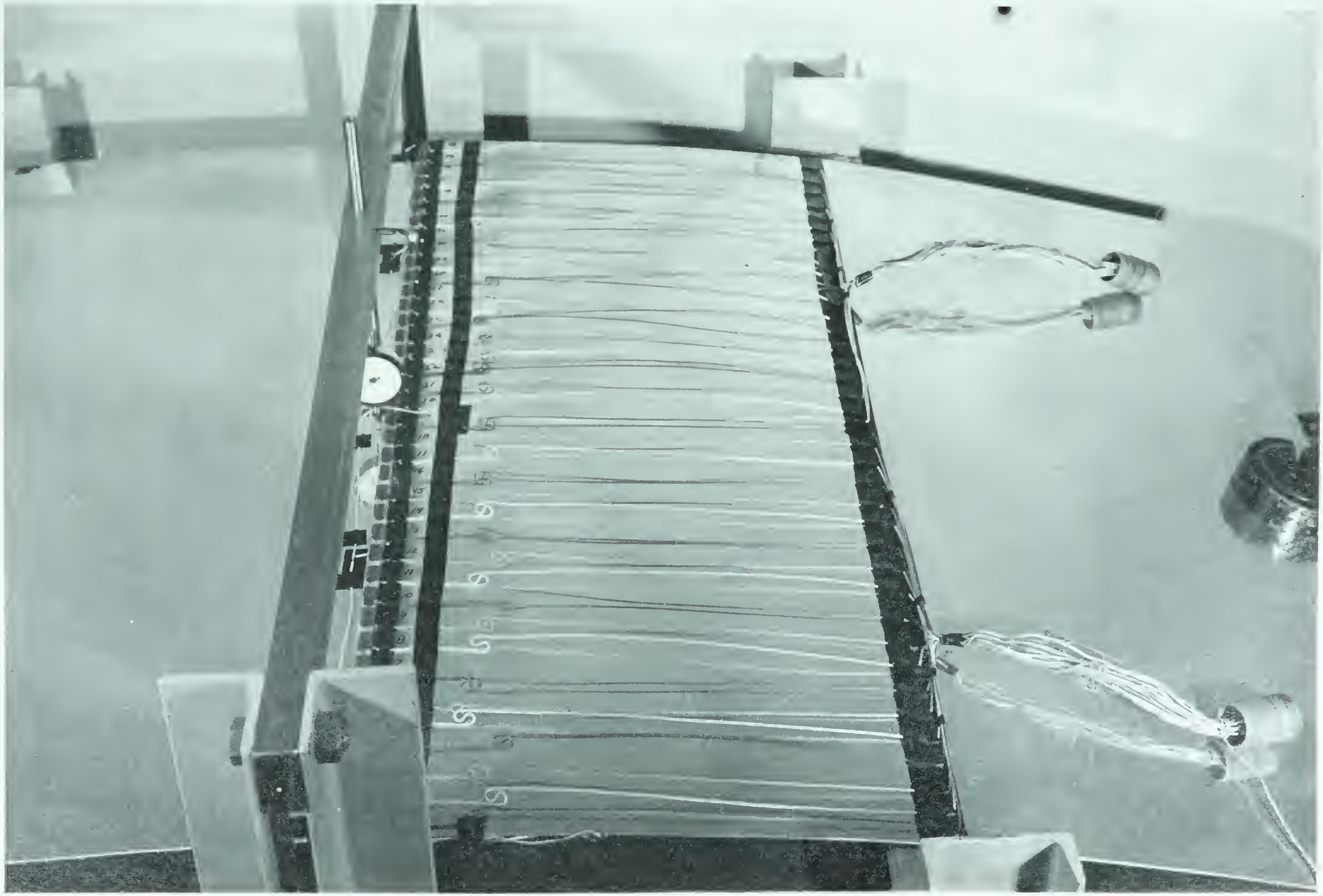

FIGURE 7. METHOD OF LOADING $\frac{1}{16} \times 38 \times 72$ INCH PLATE

reliable for reasons already given but they served as a guide in the application of the loads. In addition to the dial gauge, at the center of the plate, two strain gauges were placed back to back in the longitudinal direction to measure the longitudinal strains.

All strain gauges were "Baldwin-Lima-Hamilton SR-4" bonded filament, type A-5-1, with a resistance of 120 ohms and a gauge factor of 1.97. The A-5-1 gauge has a grid 1/2 inch long placed on a specially prepared "extra thin" paper. This type was specified for rapid elimination of the adhesive solvent and also because the thin paper allowed the gauge grid to be placed as close as possible to the plate surface.

B. Procedure

Curvature and $\frac{b^2}{Rd}$ Ratio

The testing of each plate for effect of various $\frac{b^2}{Rd}$ ratios consisted of placing the plate symmetrically on the test fixture and applying loads in suitable increments. For a particular loading, or more correctly for a particular $\frac{b^2}{Rd}$ ratio, all the strain gauges were read by means of a "Baldwin" Strain Indicator, Type NA. For each plate at least five different $\frac{b^2}{Rd}$ values were obtained. And, at least three tests were run at each ratio. The strain readings taken for each $\frac{b^2}{Rd}$ ratio were averaged.

Readings were taken as the load was applied and as the load was removed. Before a set of readings was accepted the strain gauges had to return to their initial readings after all load was removed.

Effect of Strain Gauge Paper Thickness

Appendix C describes the method in which the strain readings were converted to deflections. These calculations were based on the assumption that the strain values obtained were directly at the surface of the plate. This assumed negligible effect of the glue plus paper thickness which actually existed between the gauge grid and the plate surface. The following test was conducted to measure the effect, if any, of this thickness.

A "Mercer" dial gauge, with the return spring removed, which could be read to the nearest 0.0001 inch, was set up in the middle of the plate as shown in Figure 8. The strains in the longitudinal direction were recorded for various deflections on the dial gauge. The radius of curvature R was calculated from the dial gauge readings and compared to R calculated from the longitudinal strains. The calculations of R based on strain readings were made first, neglecting paper and glue thickness and, second, including it. For the latter, it was necessary to determine the glue and paper thickness. This was accomplished by gluing pieces of "SR-4" paper to the aluminum using the usual procedure for applying gauges and, after drying, measuring the total thickness of aluminum, glue and paper using a micrometer. It should be noted that the

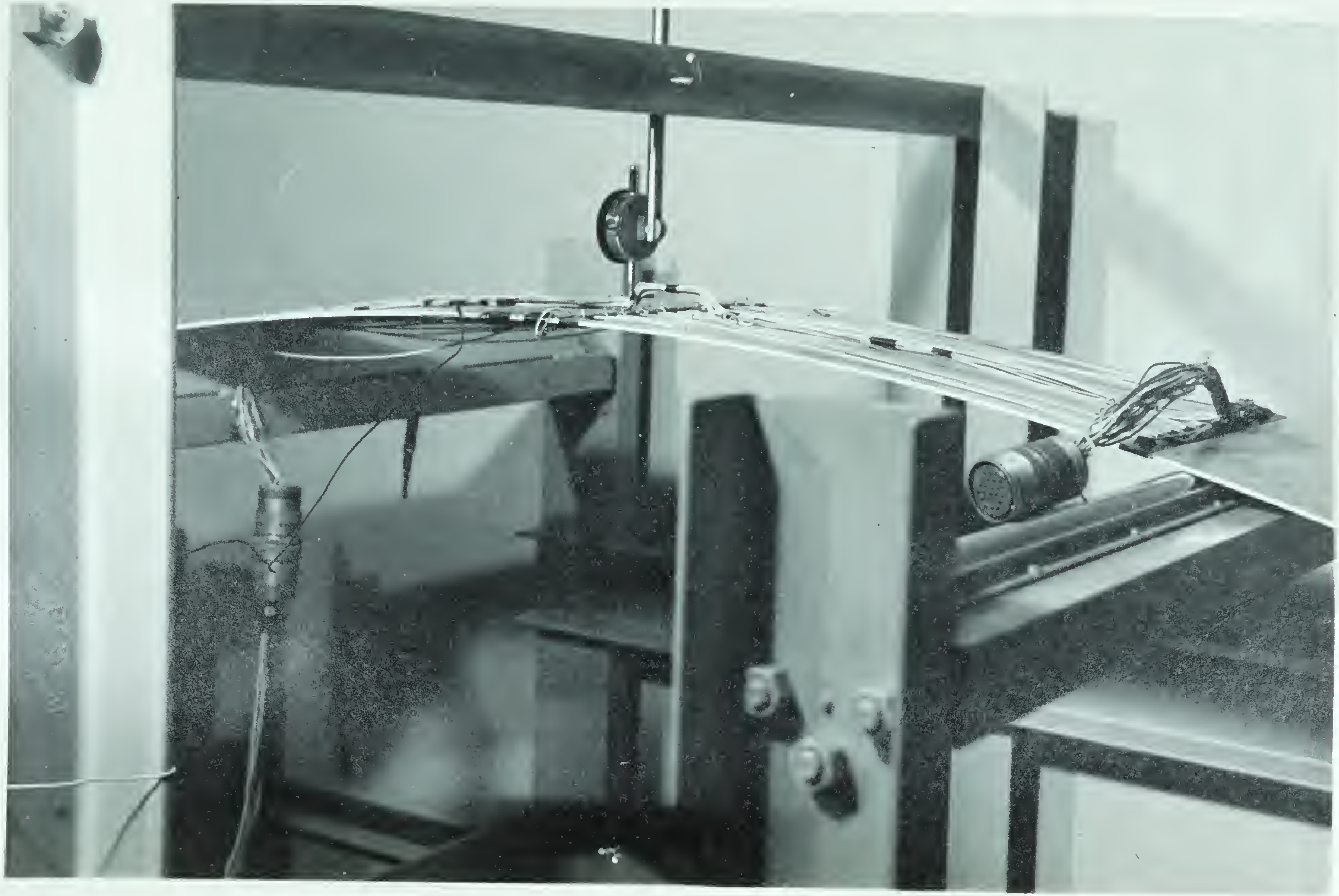

FIGURE 8. LOCATION OF "MERCER" DIAL GAUGE TO CHECK EFFECT OF PAPER PLUS GLUE THICKNESS

foregoing comparison depends upon the dial gauge readings, which, at best are not too reliable. However, it was believed that this method was the best available.

Mechanical Properties of Alclad 75 ST-6

Samples of aluminum from all the plates tested were machined to a suitable size for tensile testing in a "Baldwin" tester. Strain gauges were placed back to back on the specimen surface; one pair in the longitudinal direction and the other pair in the transverse direction. Figure 9 shows the specimen size and the location of the strain gauges. By loading in increments it was possible to test for E (Young's Modulus of Elasticity), and ν (Poisson's Ratio).

Saint-Venant's Principle

On the 1/8 x 10 x 72 inch plate strain gauges were placed longitudinally back to back on the aluminum surface every 2 inches between the fixed edge support and the plate mid-line as shown in Figure 10. These strain gauges were read for various plate deflections. If the longitudinal curvature is a constant, i.e., pure bending, all the strain gauges in the longitudinal direction will read the same for a particular loading. If all the strain readings are not identical then it can be assumed that these readings are influenced by the method of loading or the local disturbance caused by the support. This method should determine the distance away from the support at which all the strain gauge

readings are identical and, thus, determine the limits for Saint-Venant's Principle.

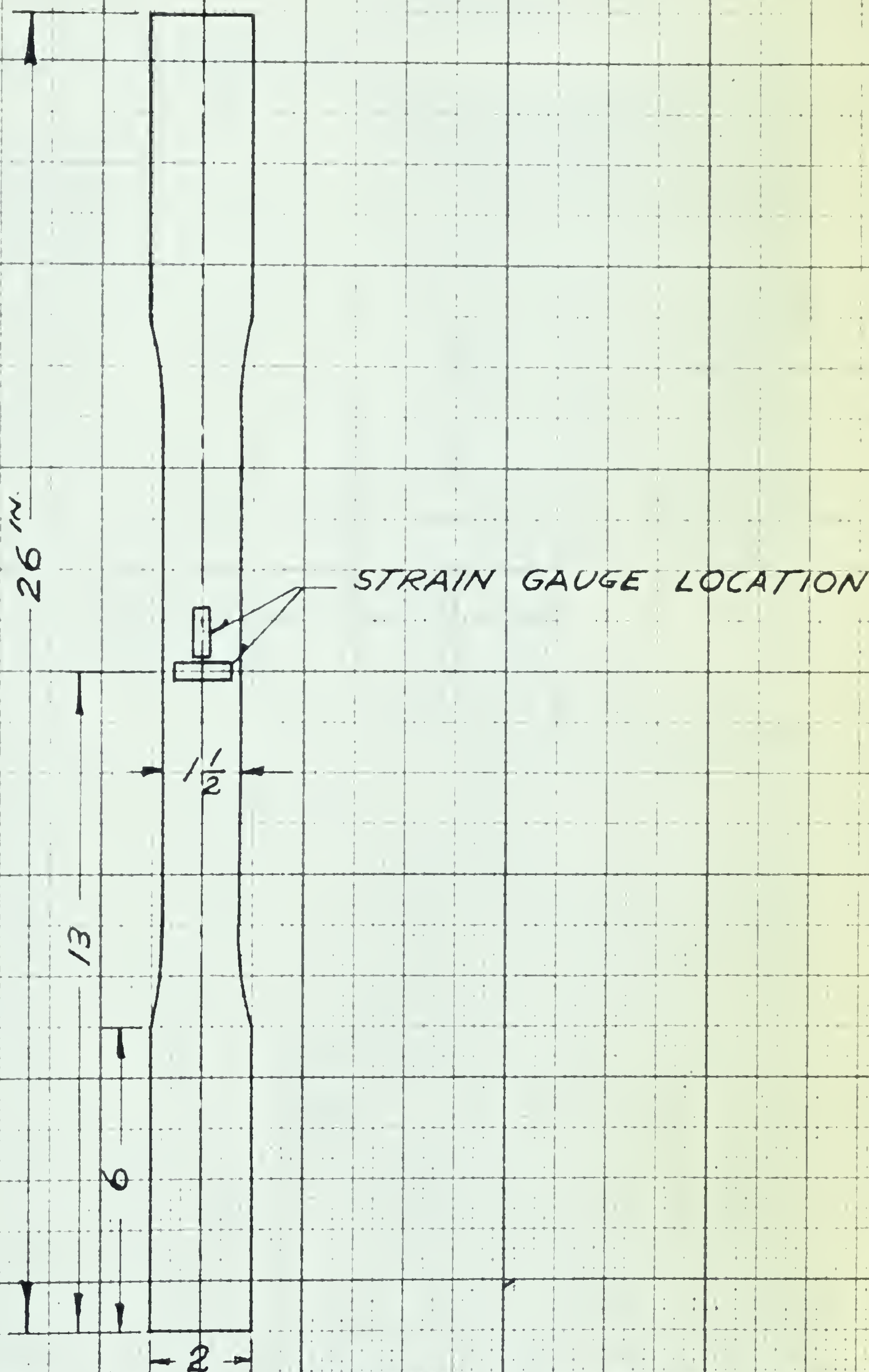

TENSILE SPECIMEN
WITH
LOCATION OF SR-4 STRAIN GAUGES

FIGURE 9

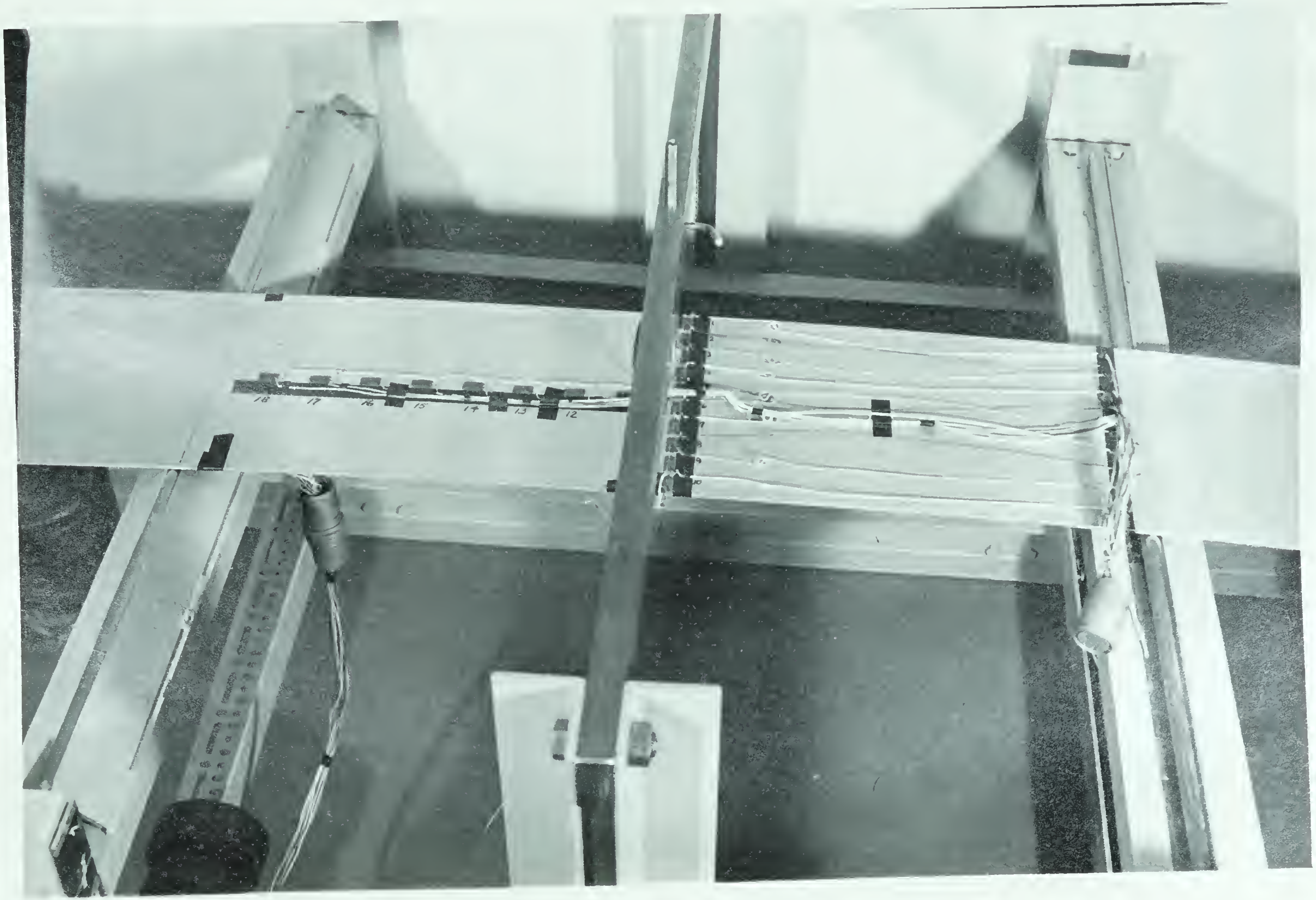

FIGURE 10. CHECKING OF SAINT-VENANT'S PRINCIPLE BY LONGITUDINALLY PLACED STRAIN GAUGES

Chapter 4 - RESULTS AND DISCUSSION

Transverse Curvature

Strain gauge readings in the transverse direction taken on each plate were plotted for various $\frac{b^2}{Rd}$ ratios. These are shown in Figures 11-24. From these curves it may be observed that the shape of the transverse strain curves, for each plate, were similar to the other plates for equivalent $\frac{b^2}{Rd}$ values. It was, therefore, believed that $\frac{b^2}{Rd}$ is a true physical ratio and that it would be a sufficient analysis to observe the slope and deflection curves for a single plate thickness. The transverse strain curves were graphically integrated twice for the 1/8 inch thick plates. The first integration gave the slope $\frac{dy}{dx}$ versus x. These curves have been plotted in Figures 25-28. The second integration gave the deflection y versus x . These curves have been plotted in Figures 29-32. Since the transverse strain curves were reasonably symmetrical, only one half of each curve was integrated.

Although the 1/8 inch thick plates behaved in a symmetrical manner, the other plates (i.e., 1/4 x 38 x 72, 3/16 x 38 x 72, 1/16 x 38 x 72) tended to deflect unsymmetrically. In particular, the 1/16 inch plate was extremely flexible and had a tendency to buckle when handled. It was believed, therefore, that the inconsistencies in the transverse strains for the 38 inch plates (in particular

with the 1/16 inch thick plate, see Figures 19 and 20) were due to the plate having distorted previously to testing.

The curves of transverse strain indicate that $\frac{b^2}{Rd}$ is a true physical ratio. Moreover, this ratio predicts the mode of the transverse strain behaviour. Referring to Figures 11-24, all strain curves with $\frac{b^2}{Rd} < 16$ have a positive slope. For $\frac{b^2}{Rd} > 22$ the curves then deviate from curves whose slopes are positive to curves whose slopes alternate from positive to negative. These curves ($\frac{b^2}{Rd} > 22$) are similar to a cosine wave which is damped as it approaches the plate center. Love (10) discusses this problem and suggests that the strain in the middle surface, for a radius of curvature R of the same order of magnitude as the width, follows a cosine function which is damped towards the center of the plate.

The experimental work contained herein indicated that the behaviour of the transverse strain is related to the dimensionless ratio $\frac{b^2}{Rd}$. Also, the mode of the strain curves change for $16 < \frac{b^2}{Rd} < 22$.

The curves of deflection y versus x (see Figures 29-32) also behave according to the $\frac{b^2}{Rd}$ ratio. These curves show for $\frac{b^2}{Rd} < 24$ the deflection at the edge is positive. For $\frac{b^2}{Rd} > 24$ the deflection at the edge becomes negative. Hence, for $\frac{b^2}{Rd} > 24$ the center of the plate is higher than

the edge. This means the transverse curvature becomes synclastic for values of $\frac{b^2}{Rd} > 24$. The transformation, then, is from anticlastic behaviour to synclastic behaviour. It is also evident from the deflection curves that nowhere does a transverse strip remain flat. These observations apparently contradict Ashwell and Fung and Wittrick, who maintain for $\frac{b^2}{Rd} > 100$ the plate, in the transverse direction, remains essentially flat except at the boundaries where there is a slight edge effect. Values of $\frac{b^2}{Rd}$ as high as 191 were recorded and from the deflection curves it can be seen that no portion of the transverse strip remains flat.

It is very possible that the discrepancies between the experimental work of this thesis and the accepted theory is due to the plates having small initial strains. According to Ashwell (5) " .... the type of distortion concerned was extremely sensitive to the presence of these (initial) strains."

Effect of Strain Gauge Paper Thickness

The radius of curvature R, in the longitudinal direction, was plotted for different plate loadings as shown in Figure 33. Three curves were plotted. One curve shows R calculated from dial gauge readings. The other two curves of R were obtained from strain gauges; one curve assuming negligible paper plus glue thickness, the other considering

a paper plus glue thickness of 0.011 inch, i.e., assuming strains recorded were the strains 0.011 inch from the plate surface rather than surface strains.

Figure 33 shows that the curve of R calculated from the dial gauge, for the range tested, lies approximately mid-way between the two curves which were obtained from strain gauges. Thus, there was no reason for, or against, neglecting the strain gauge paper plus glue thickness. For convenience, all calculations were made neglecting the paper plus glue thickness.

Mechanical Properties of Alclad 75 ST-6

Stress strain values were plotted for all aluminum tensile specimens tested as in Figure 35. A single curve was drawn through the majority of the plotted points. The slope of this curve (the modulus of elasticity) was found to be equal to 10×10^6 lbs/in^2. In a similar manner Poisson's Ratio was found to be equal to 0.31 (see Figure 36). The manufacturer gives $E = 10.4 \times 10^6$ lbs/in^2 for this alloy.

Since the plotted experimental points of each plate tested lie close to one another, it can be said that all aluminum plates had the same mechanical properties. This justifies an original assumption that, regardless of thickness, all plates of aluminum would behave in a like manner for a particular $\frac{b^2}{Rd}$ value.

Saint-Venant's Principle

For the 1/8 x 10 x 72 inch plate values of strain versus the longitudinal distance from the plate center were plotted for different $\frac{b^2}{Rd}$ values as shown in Figure 34. For each $\frac{b^2}{Rd}$ value the spread between longitudinal strain readings was less than 4 percent. A straight "best fit" line was used to connect the plotted readings.

Since the longitudinal strains were constant for a particular deflection the longitudinal curvature was cylindrical. The significant point from this test was that Gauge No. 18 (2 inches away from the fixed support) did not register any irregular readings when compared to the other gauges. Hence the effect of the local disturbance set up by the fixed support could not be detected by a strain gauge 2 inches away from the local disturbance. The assumption that Saint-Venant's Principle is valid for the size of plates chosen and the method of loading is, thus, justified.

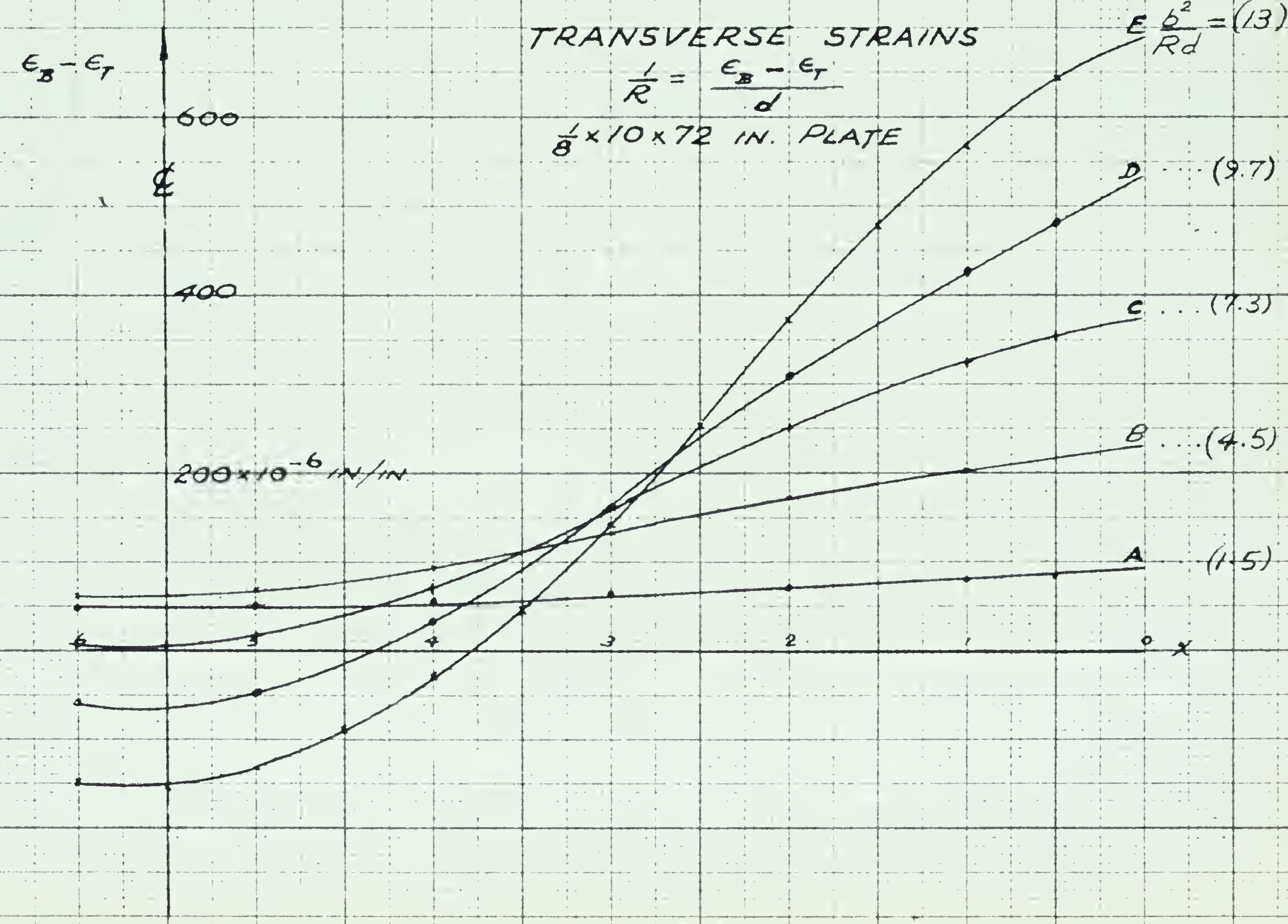
TRANSVERSE STRAINS
$\frac{1}{R} = \frac{\epsilon_B - \epsilon_T}{d}$
$\frac{1}{8} \times 10 \times 72$ IN. PLATE
$\epsilon_B - \epsilon_T$
600
400
200×10^{-6} IN/IN
E $\frac{b^2}{Rd} = (13)$
D ... (9.7)
C ... (7.3)
B ... (4.5)
A ... (1.5)
6
5
4
3
2
1
0
X

FIGURE 11.

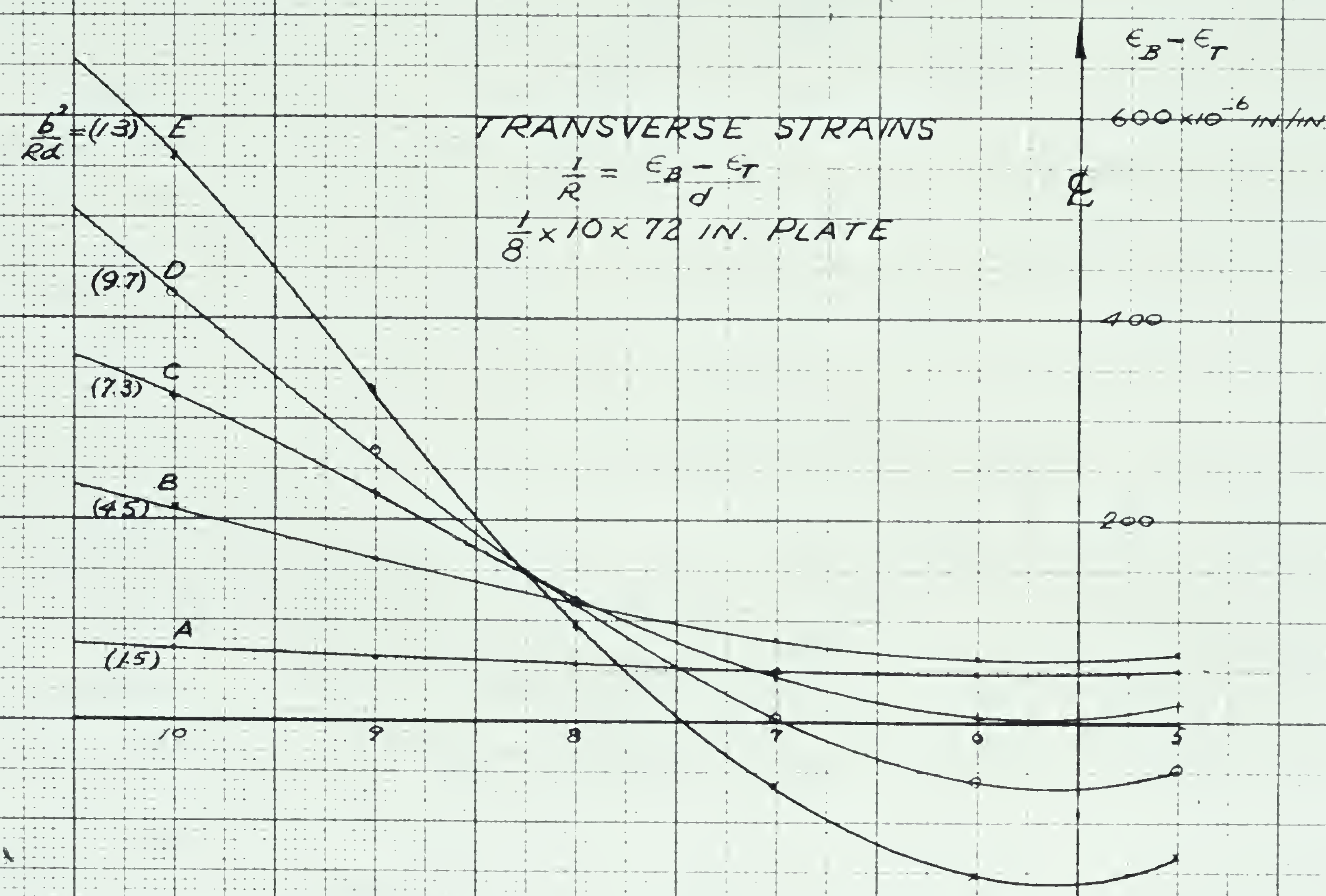
$\epsilon_B - \epsilon_T$
600×10^{-6} IN/IN.
400
200
TRANSVERSE STRAINS
$\frac{1}{R} = \frac{\epsilon_B - \epsilon_T}{d}$
$\frac{1}{8} \times 10 \times 72$ IN. PLATE
$\frac{b^2}{Rd} = (13)$ E
(9.7) D
(7.3) C
(4.5) B
(1.5) A
10
9
8
7
6
5

FIGURE 12

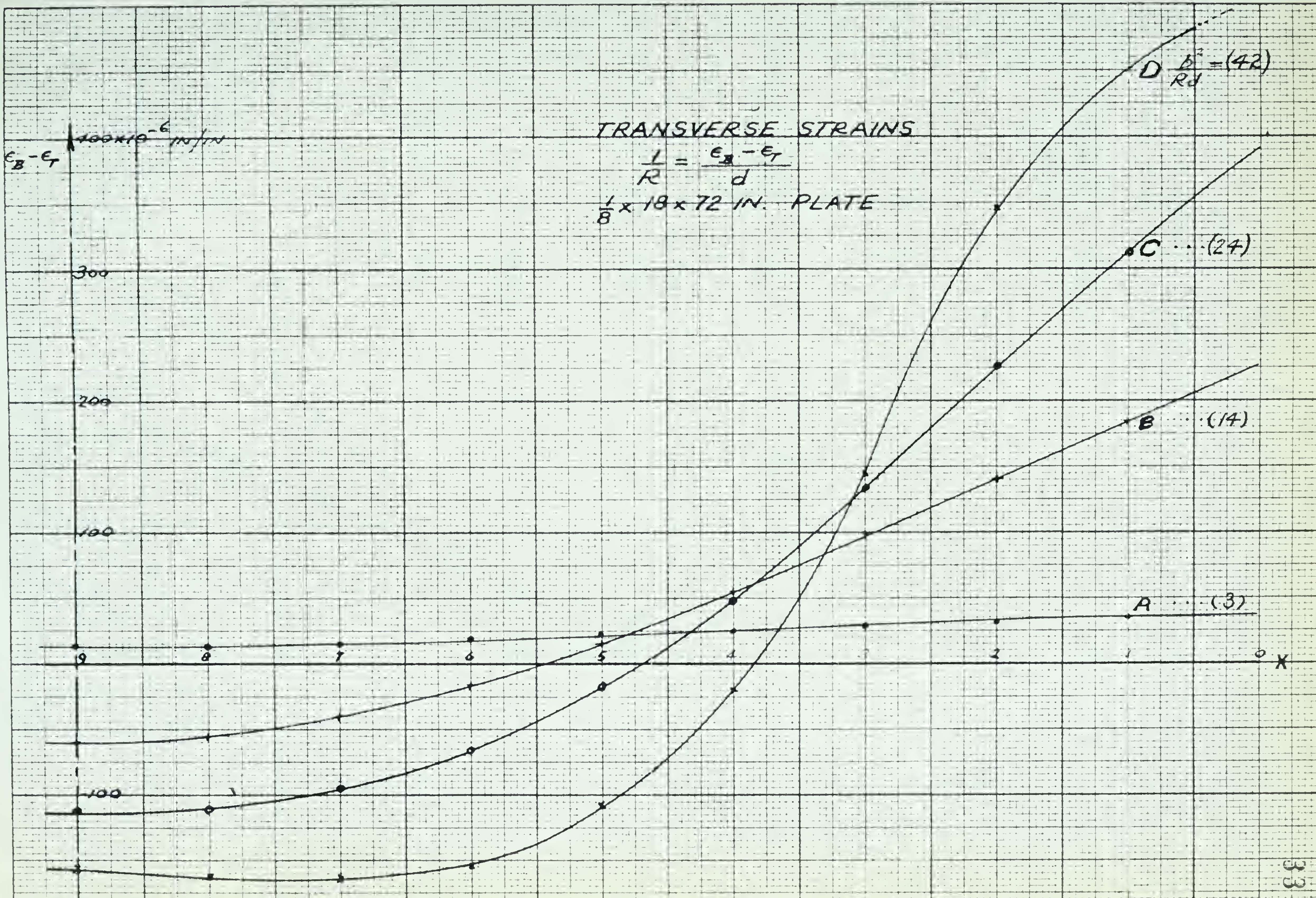
TRANSVERSE STRAINS
$\frac{1}{R} = \frac{\epsilon_B - \epsilon_T}{d}$
$\frac{1}{8} \times 18 \times 72$ IN. PLATE
$\epsilon_B - \epsilon_T$
100×10^{-6} IN/IN
300
200
100
100
9
8
7
6
5
4
3
2
1
0
X
D $\frac{b^2}{Rd}$ = (42)
C ... (24)
B ... (14)
A ... (3)

FIGURE 13

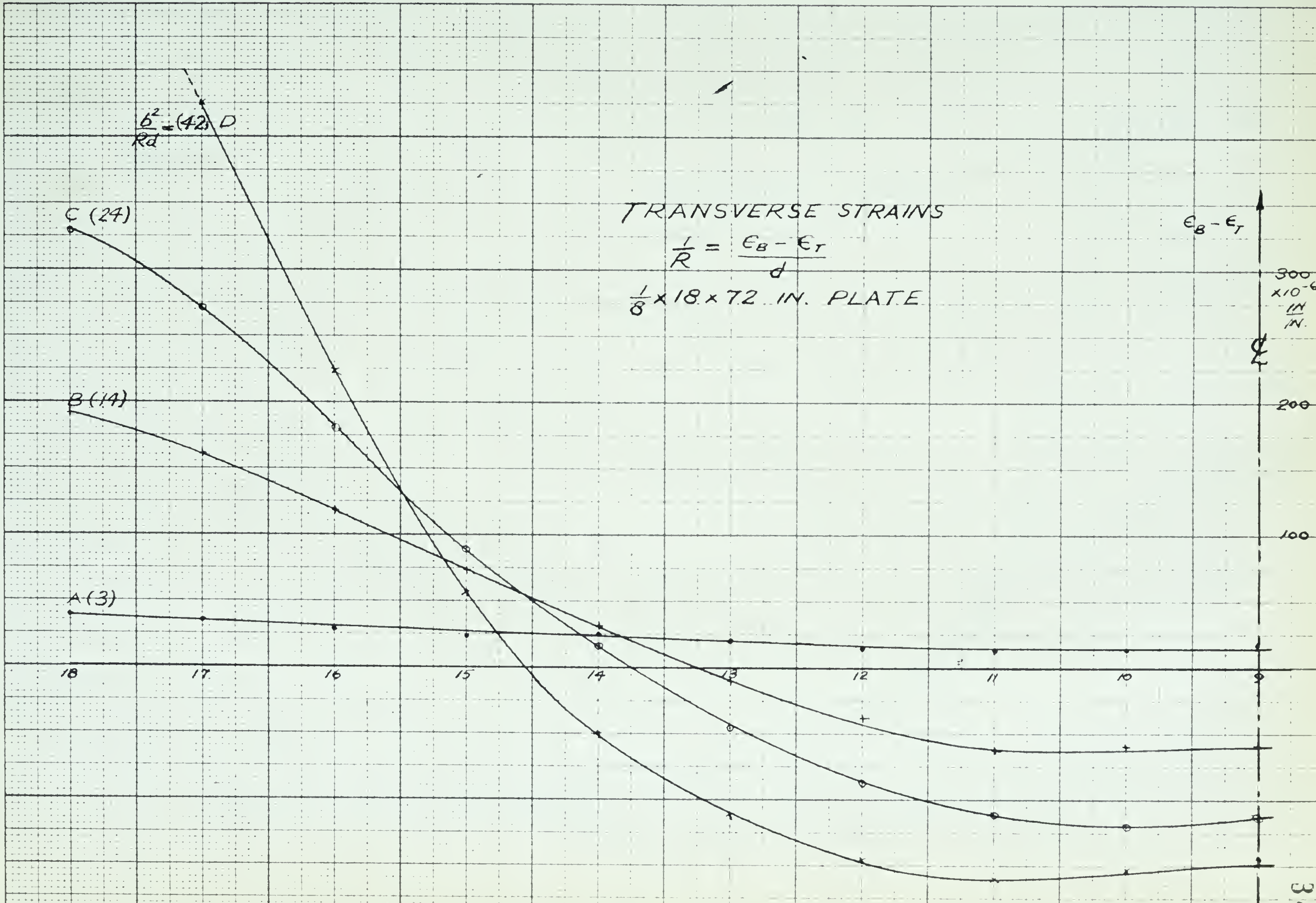
TRANSVERSE STRAINS
$\frac{1}{R} = \frac{\epsilon_B - \epsilon_T}{d}$
$\frac{1}{8} \times 18 \times 72$ IN. PLATE
$\epsilon_B - \epsilon_T$
300
$\times 10^{-6}$ $\frac{IN}{IN.}$
200
100
℄
$\frac{b^2}{Rd} = (42)$ D
C (24)
B (14)
A (3)
18
17
16
15
14
13
12
11
10
9

FIGURE 14

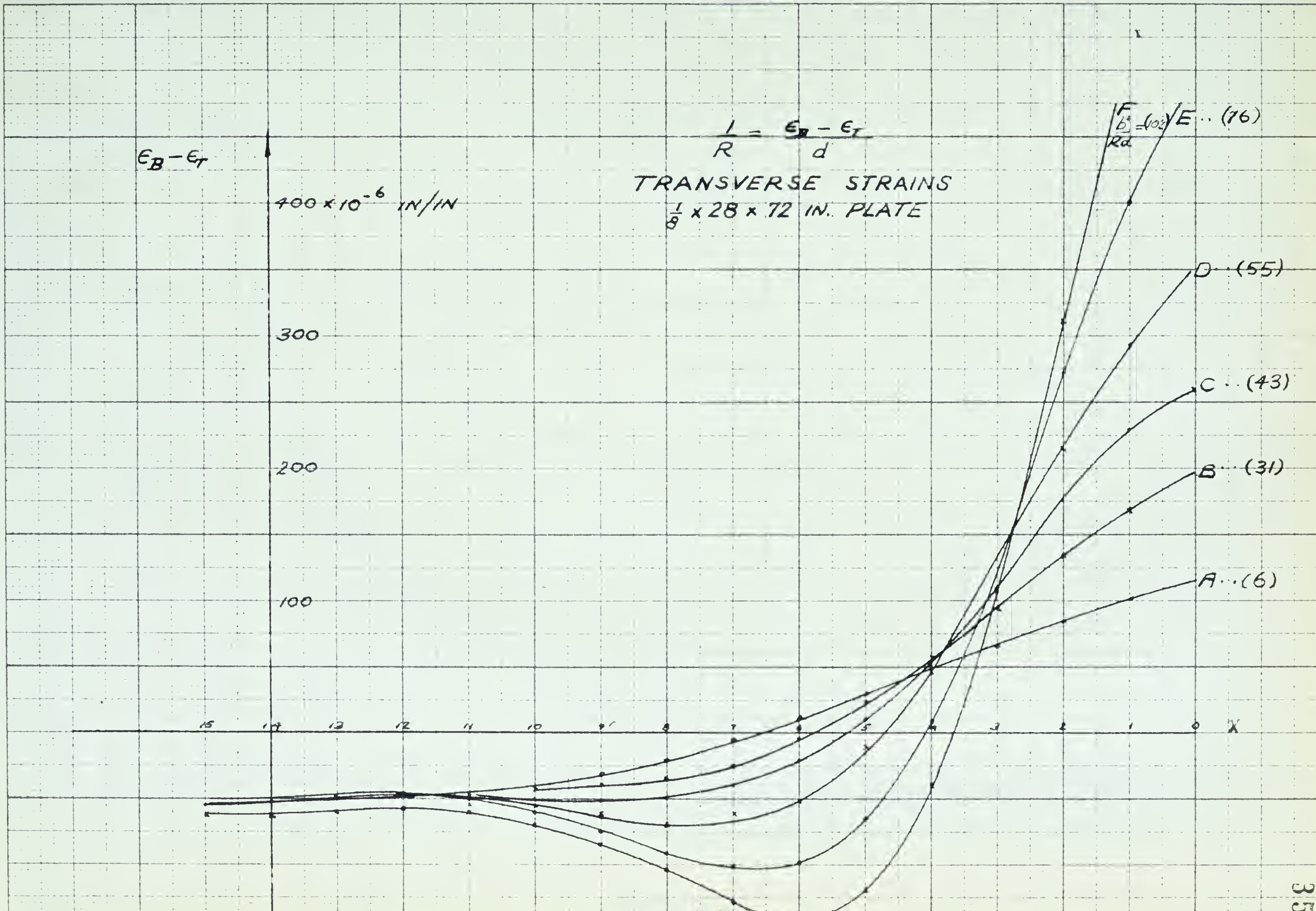

$\epsilon_B - \epsilon_T$
400 × 10^-6 IN/IN
300
200
100
$\frac{1}{R} = \frac{\epsilon_B - \epsilon_T}{d}$
TRANSVERSE STRAINS
1/8 × 28 × 72 IN. PLATE
E ·· (76)
D ·· (55)
C ·· (43)
B ·· (31)
A ·· (6)
X
0
1
2
3
4
5
6
7
8
10
11
12
13
14
15

FIGURE 15

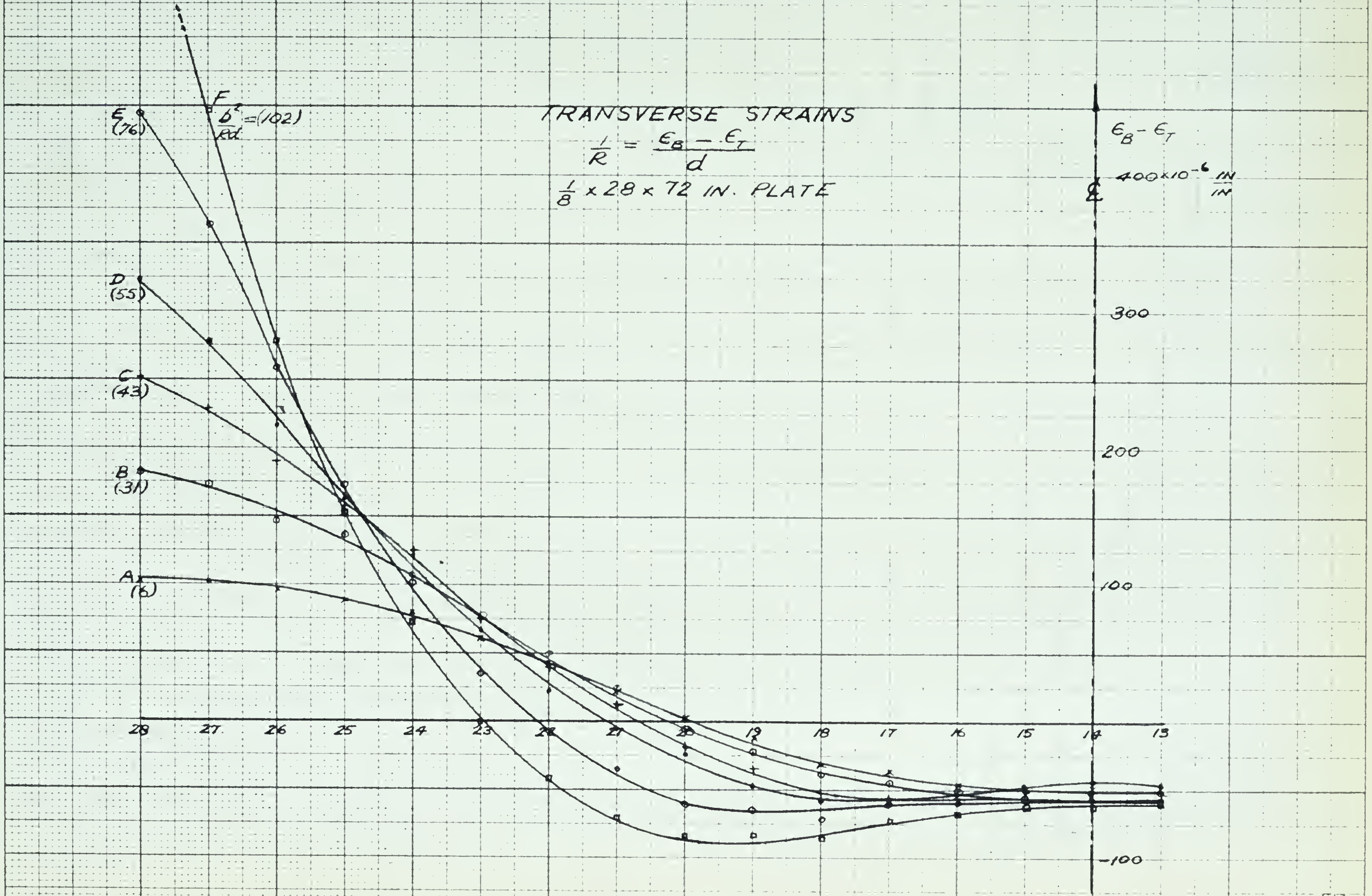

TRANSVERSE STRAINS
$\frac{1}{R} = \frac{\epsilon_B - \epsilon_T}{d}$
$\frac{1}{8} \times 28 \times 72$ IN. PLATE
$\epsilon_B - \epsilon_T$
$400 \times 10^{-6} \frac{IN}{IN}$
300
200
100
-100
28
27
26
25
24
23
22
21
20
19
18
17
16
15
14
13
F
$\frac{b^2}{Rd} = (102)$
E (76)
D (55)
C (43)
B (31)
A (16)

FIGURE 16

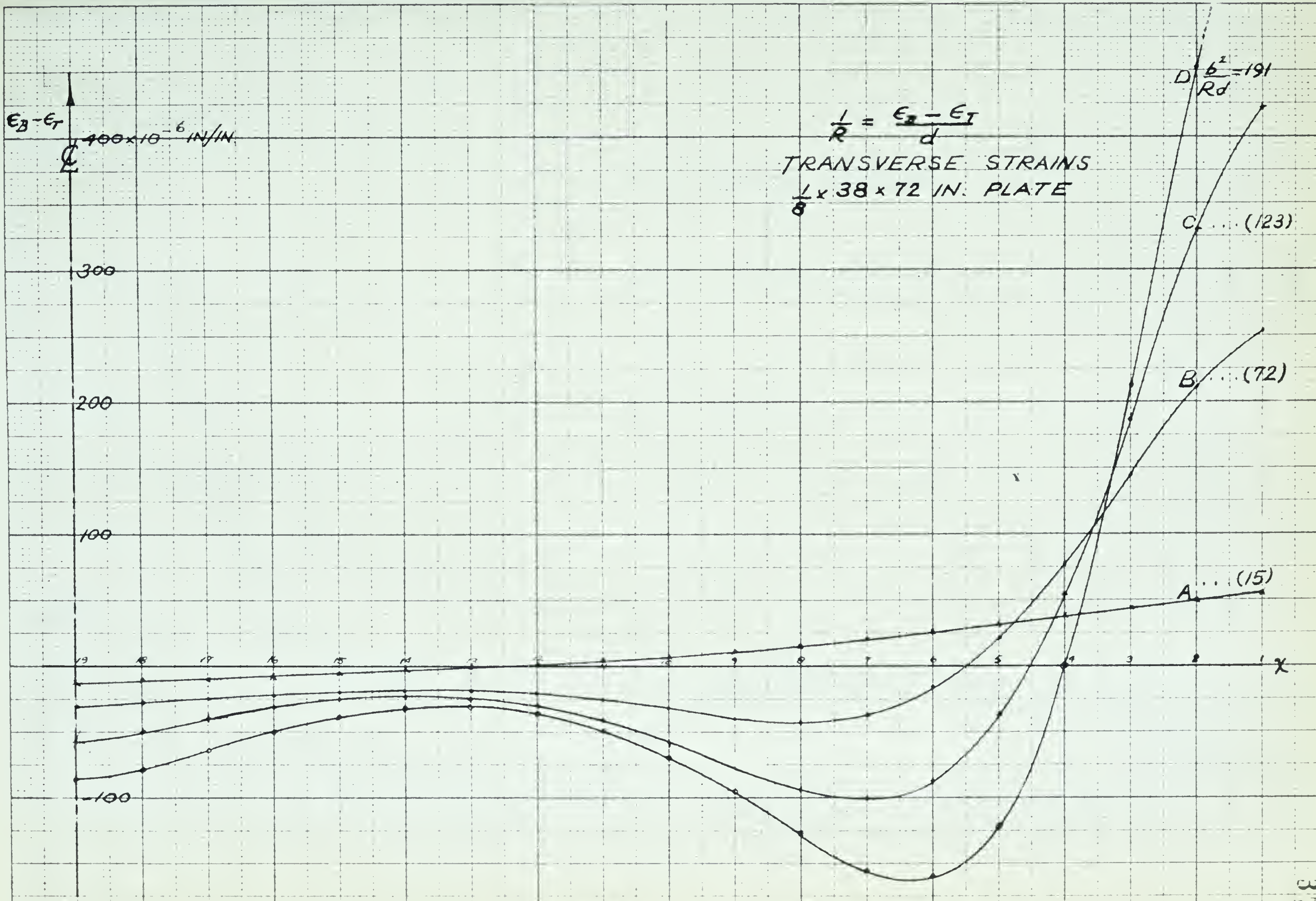
$\epsilon_B - \epsilon_T$
400×10^{-6} IN/IN
℄
300
200
100
-100
$\frac{1}{R} = \frac{\epsilon_B - \epsilon_T}{d}$
TRANSVERSE STRAINS
$\frac{1}{8} \times 38 \times 72$ IN. PLATE
D $\frac{b^2}{Rd} = 191$
C . . . (123)
B . . . (72)
A . . . (15)
X
0

FIGURE 17

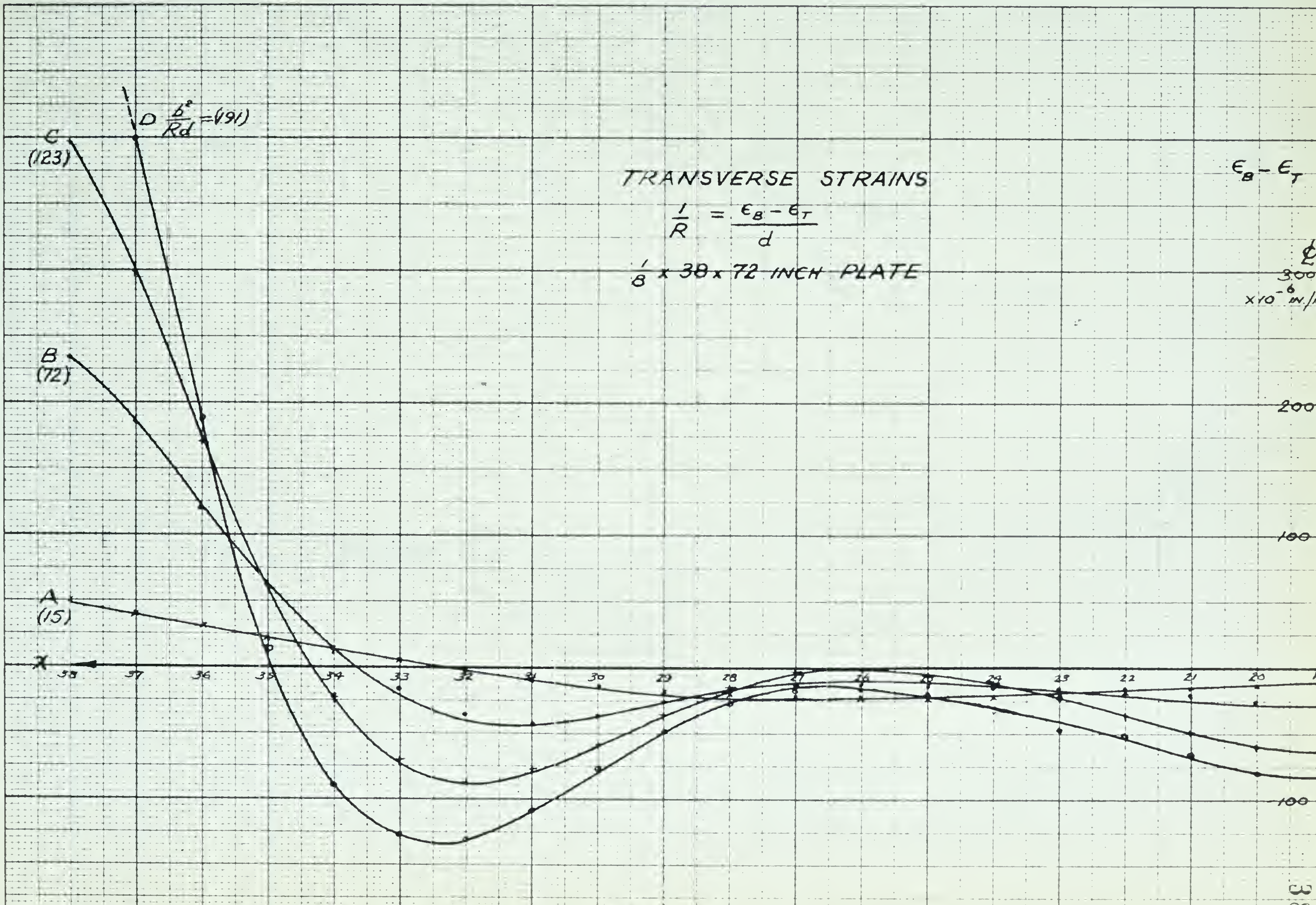
TRANSVERSE STRAINS
$\frac{1}{R} = \frac{\epsilon_B - \epsilon_T}{d}$
$\frac{1}{8}$ x 38 x 72 INCH PLATE
$\epsilon_B - \epsilon_T$
℄
300
$\times 10^{-6}$ IN./IN.
200
100
100
D $\frac{b^2}{Rd}$ = (191)
C (123)
B (72)
A (15)
X
38
37
36
35
34
33
32
31
30
29
28
27
26
25
24
23
22
21
20
19

FIGURE 18

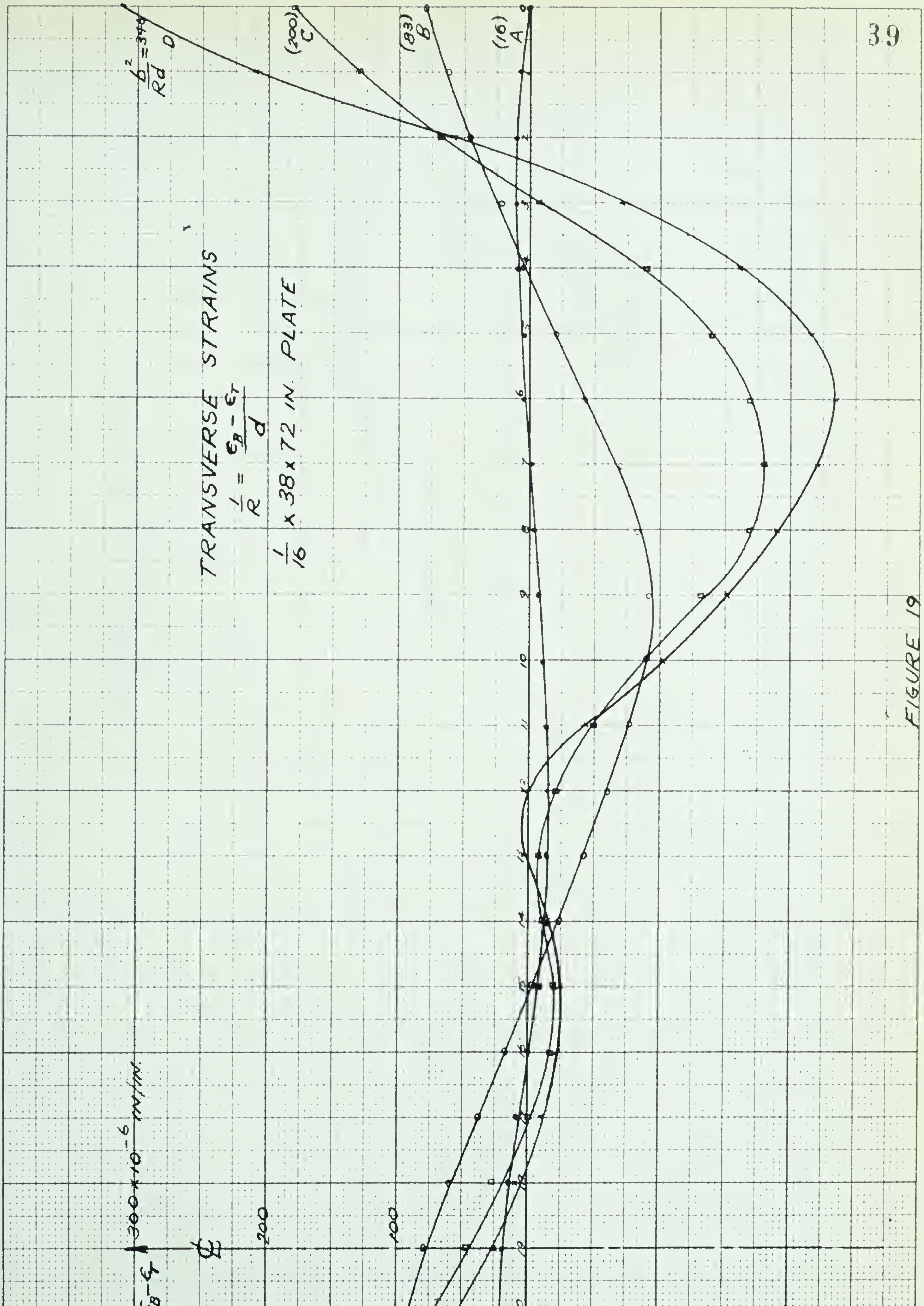

TRANSVERSE STRAINS
$\frac{1}{R} = \frac{\epsilon_B - \epsilon_T}{d}$
$\frac{1}{16}$ x 38 x 72 IN. PLATE
$\frac{b^2}{Rd} = 340$ D
(200) C
(83) B
(16) A
$\epsilon_B - \epsilon_T$ 300 x 10^{-6} IN/IN.
200
100
℄

FIGURE 19

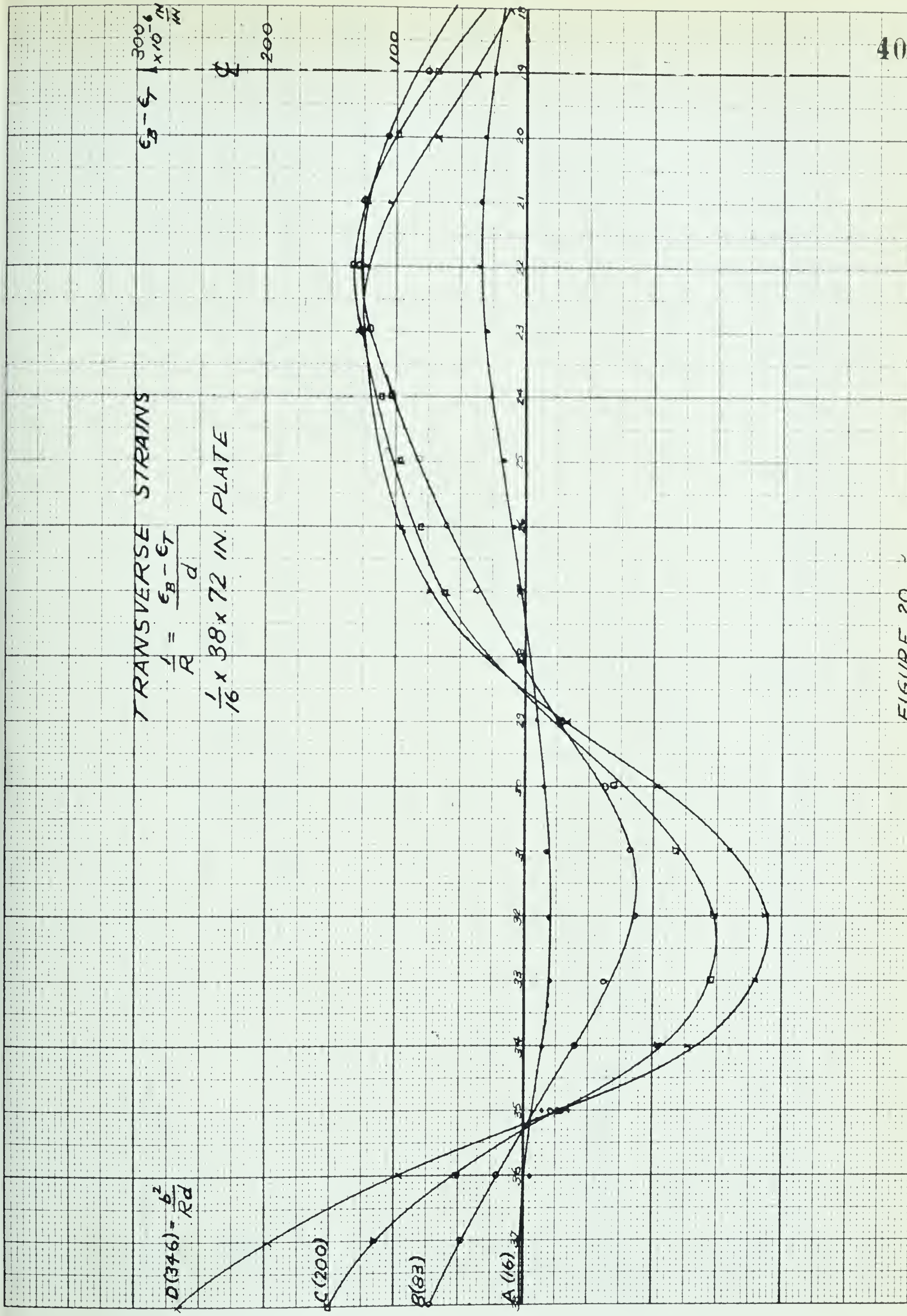
TRANSVERSE STRAINS
$\frac{1}{R} = \frac{\epsilon_B - \epsilon_T}{d}$
$\frac{1}{16} \times 38 \times 72$ IN. PLATE
$\epsilon_B - \epsilon_T$ 300×10^{-6} IN/IN
200
100
℄
D(346) = $\frac{b^2}{Rd}$
C(200)
B(83)
A(16)
18
19
20
21
22
23
24
25
26
27
28
29
30
31
32
33
34
35
36
37
38

FIGURE 20

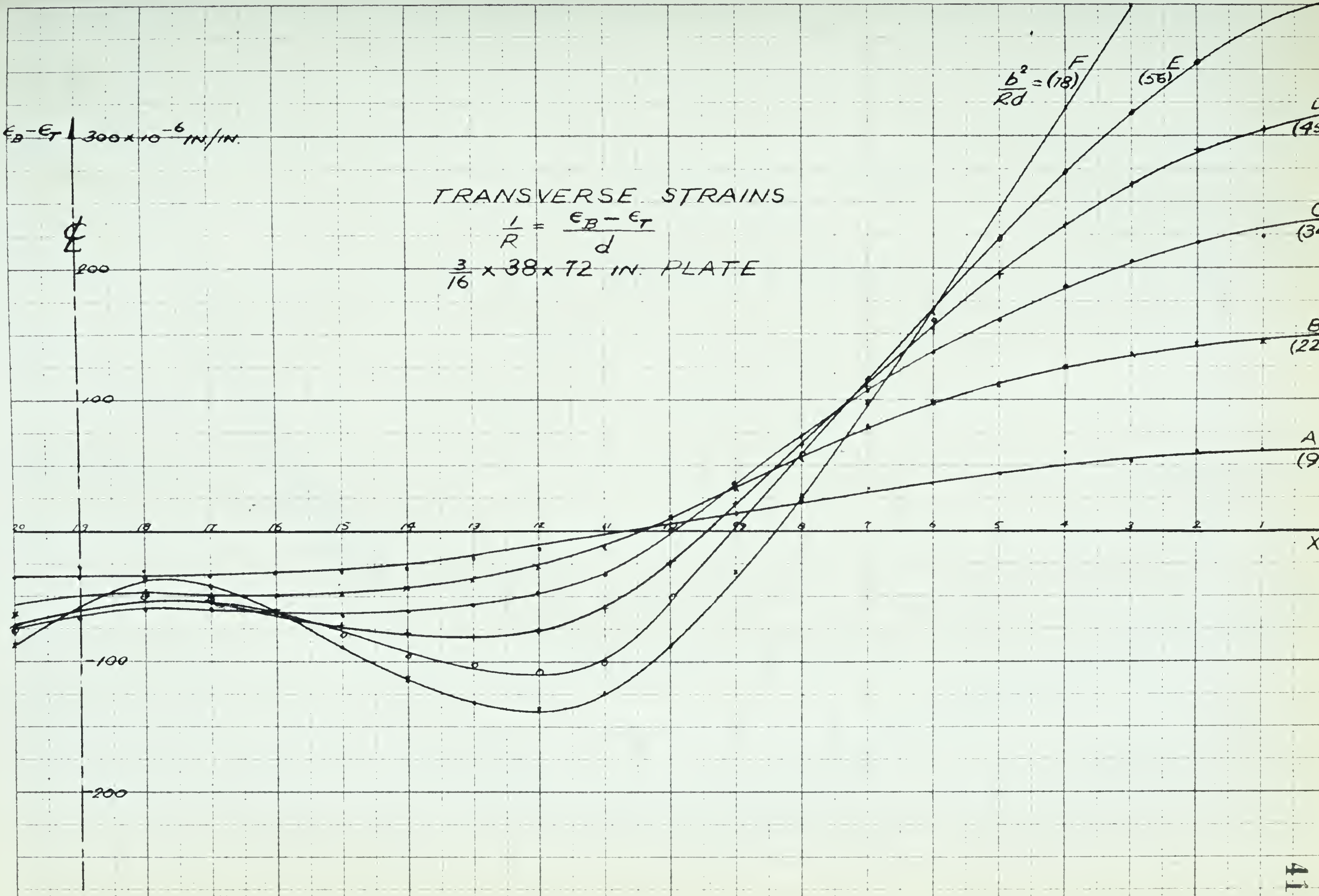

$\epsilon_B - \epsilon_T$ 300 × 10^{-6} IN./IN.
TRANSVERSE STRAINS
$\frac{1}{R} = \frac{\epsilon_B - \epsilon_T}{d}$
$\frac{3}{16}$ x 38 x 72 IN. PLATE
200
100
-100
-200
$\frac{b^2}{Rd}$ = (78) F
(56) E
D (45)
C (34)
B (22)
A (9)
X
20 19 18 17 16 15 14 13 12 11 10 9 8 7 6 5 4 3 2 1 0

FIGURE 21

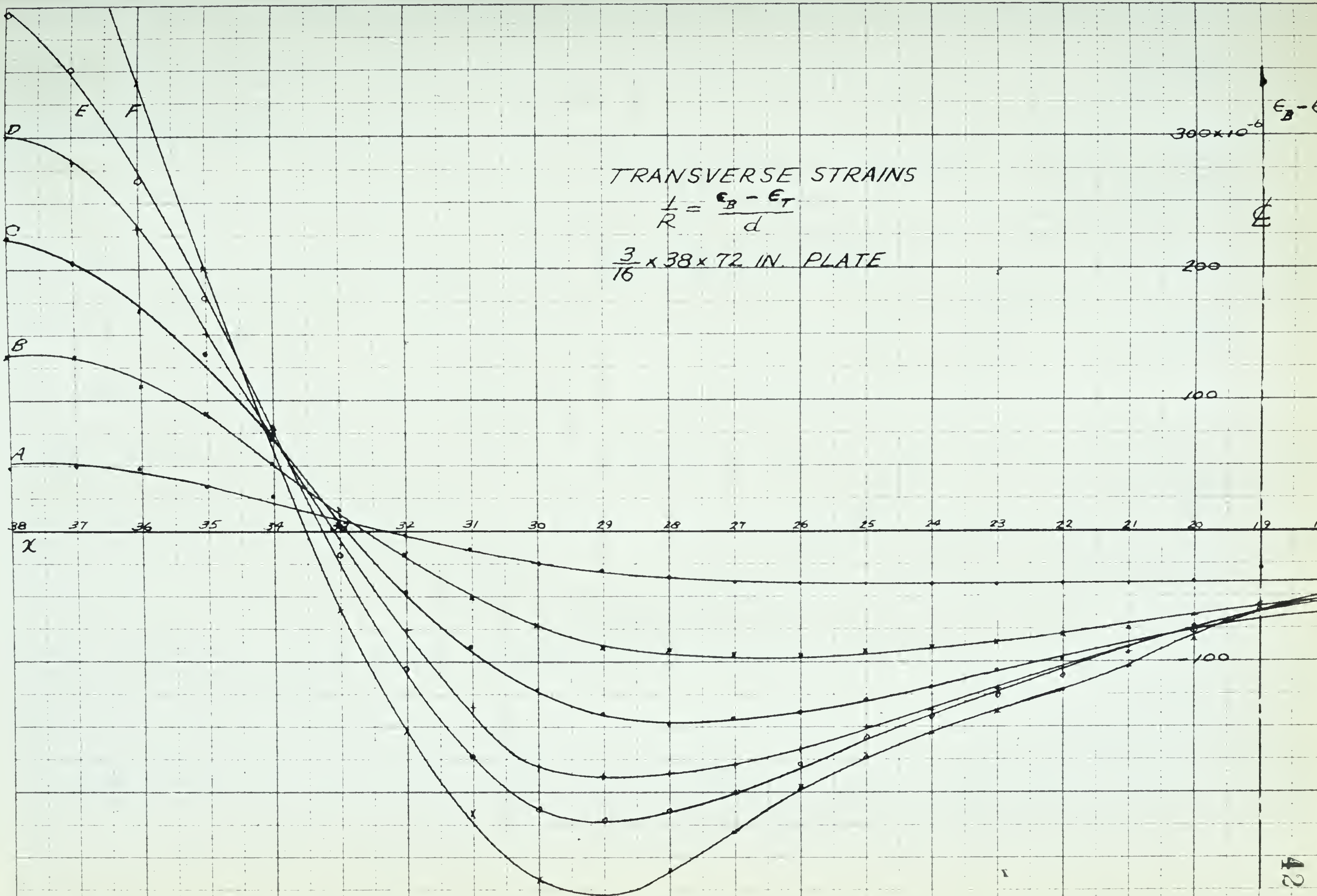
TRANSVERSE STRAINS
$\frac{1}{R} = \frac{\epsilon_B - \epsilon_T}{d}$
$\frac{3}{16} \times 38 \times 72$ IN. PLATE
$\epsilon_B - \epsilon_T$
300×10^{-6}
200
100
-100
℄
A
B
C
D
E
F
x
38
37
36
35
34
32
31
30
29
28
27
26
25
24
23
22
21
20
19
18

FIGURE 22

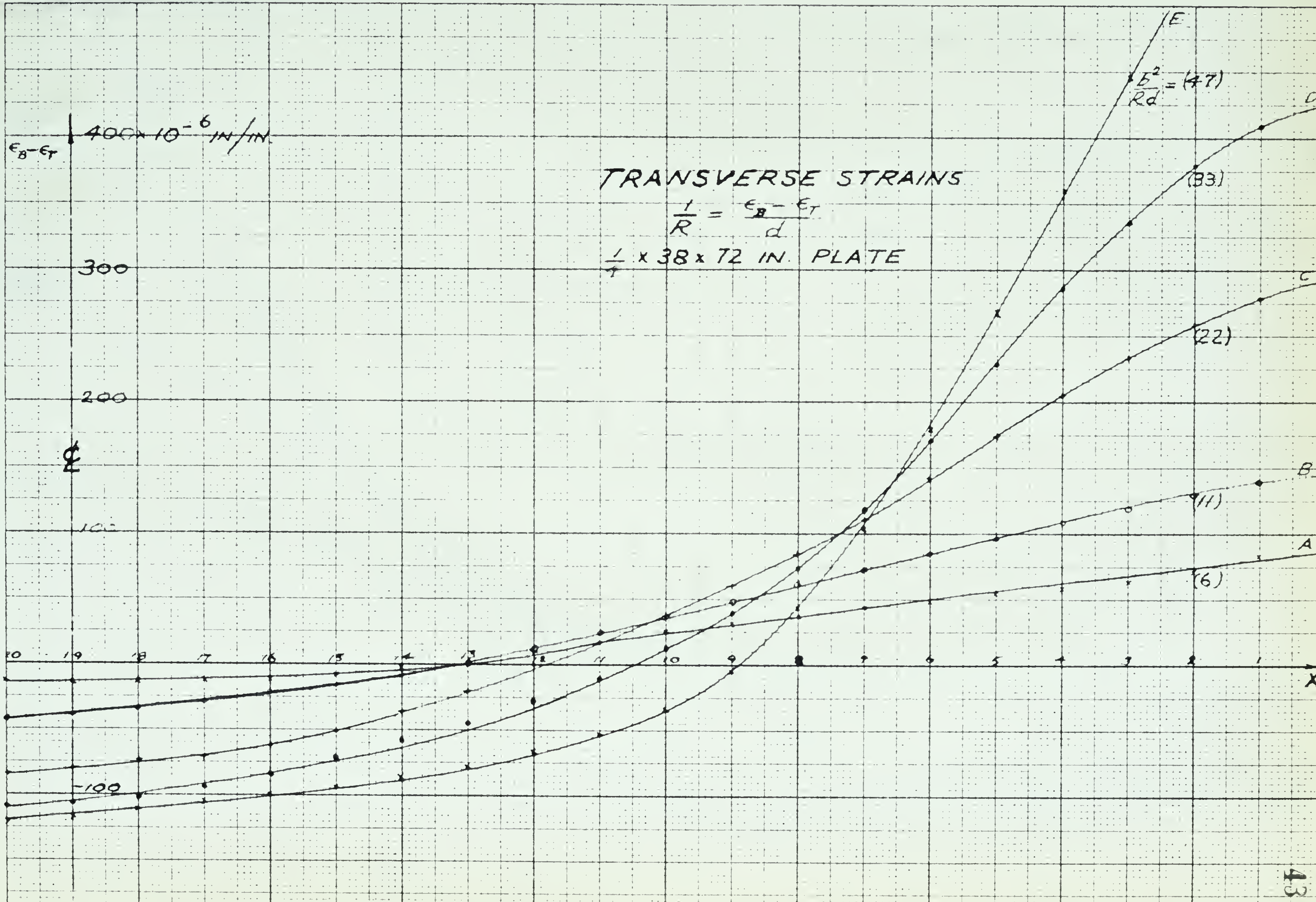

TRANSVERSE STRAINS
$\frac{1}{R} = \frac{\epsilon_B - \epsilon_T}{d}$
$\frac{1}{4}$ x 38 x 72 IN. PLATE
$\epsilon_B - \epsilon_T$
400×10^{-6} IN/IN
300
200
100
-100
-200
X
A
B
C
D
E
(6)
(11)
(22)
(33)
$\frac{b^2}{Rd} = (47)$

FIGURE 23

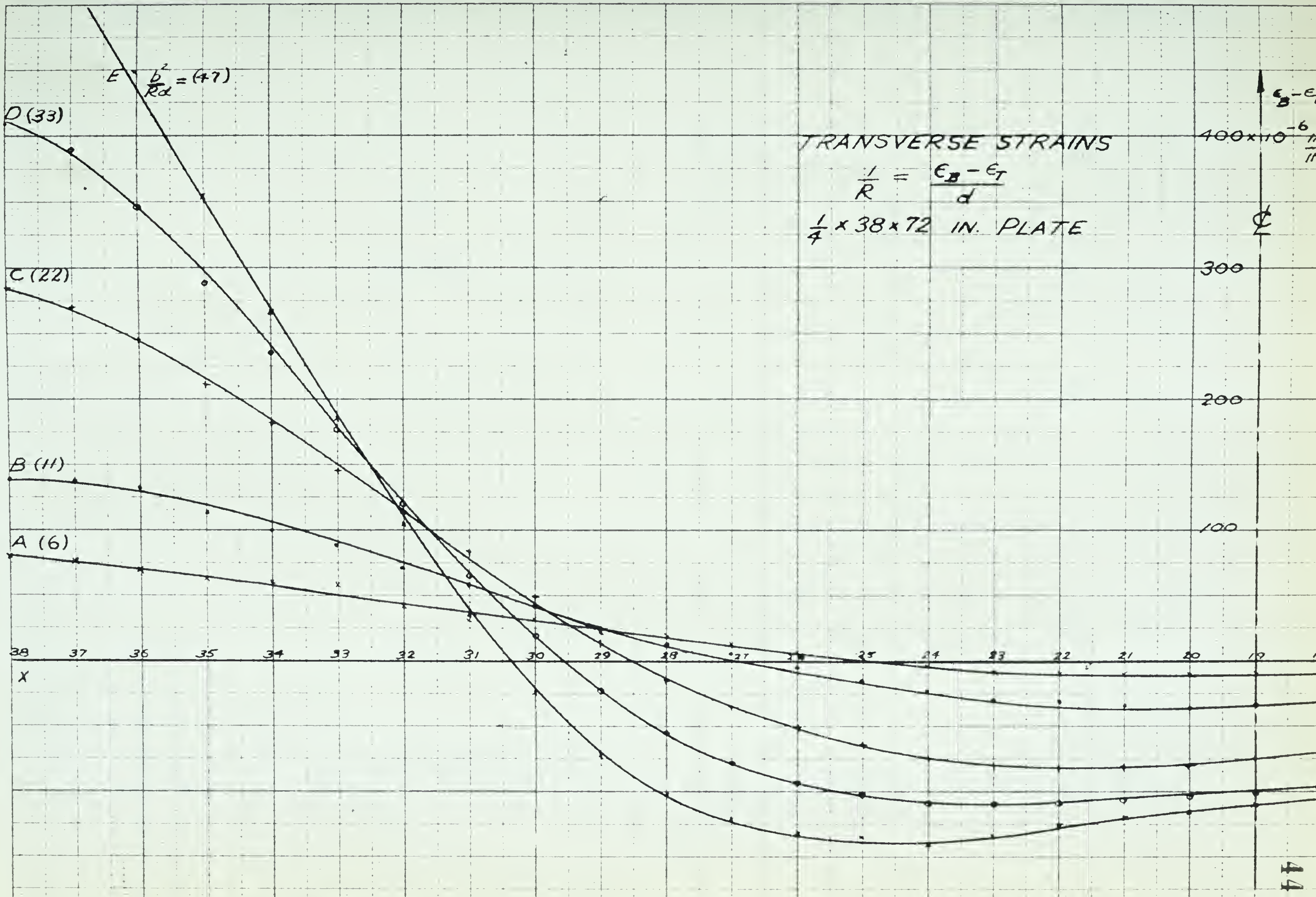
TRANSVERSE STRAINS
$\frac{1}{R} = \frac{\epsilon_B - \epsilon_T}{d}$
$\frac{1}{4} \times 38 \times 72$ IN. PLATE
$\epsilon_B - \epsilon_T$
$400 \times 10^{-6} \frac{IN}{IN}$
300
200
100
℄
$E \quad \frac{b^2}{Rd} = (47)$
D (33)
C (22)
B (11)
A (6)
38
37
36
35
34
33
32
31
30
29
28
27
26
25
24
23
22
21
20
19
18
X

FIGURE 24

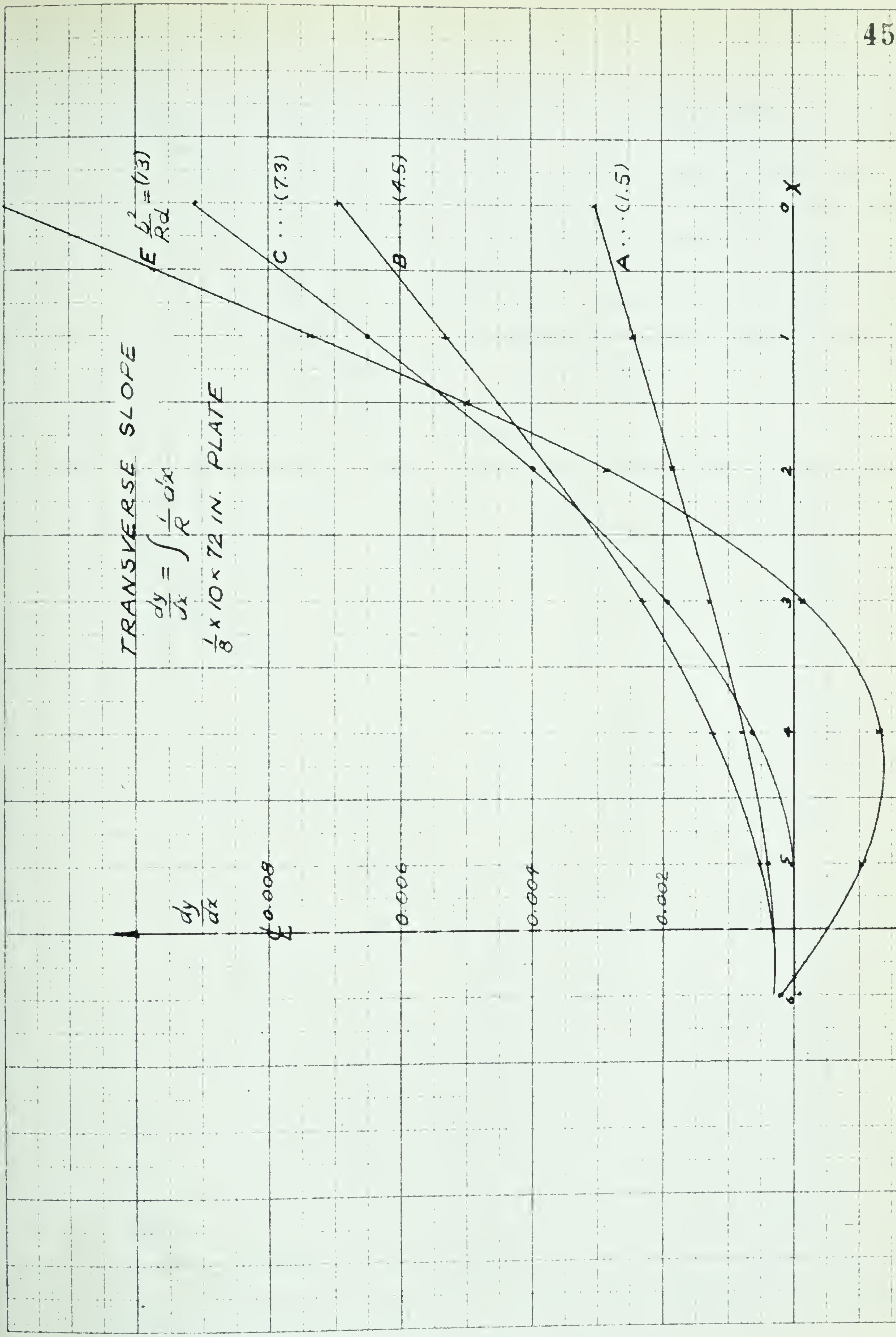

TRANSVERSE SLOPE
$\frac{dy}{dx} = \int \frac{1}{R} dx$
$\frac{1}{8} \times 10 \times 72$ IN. PLATE
E $\frac{b^2}{Rd} = (13)$
C . . . (7.3)
B . . . (4.5)
A . . . (1.5)
$\frac{dy}{dx}$
0.008
0.006
0.004
0.002
X
0
1
2
3
4
5
6

FIGURE 25

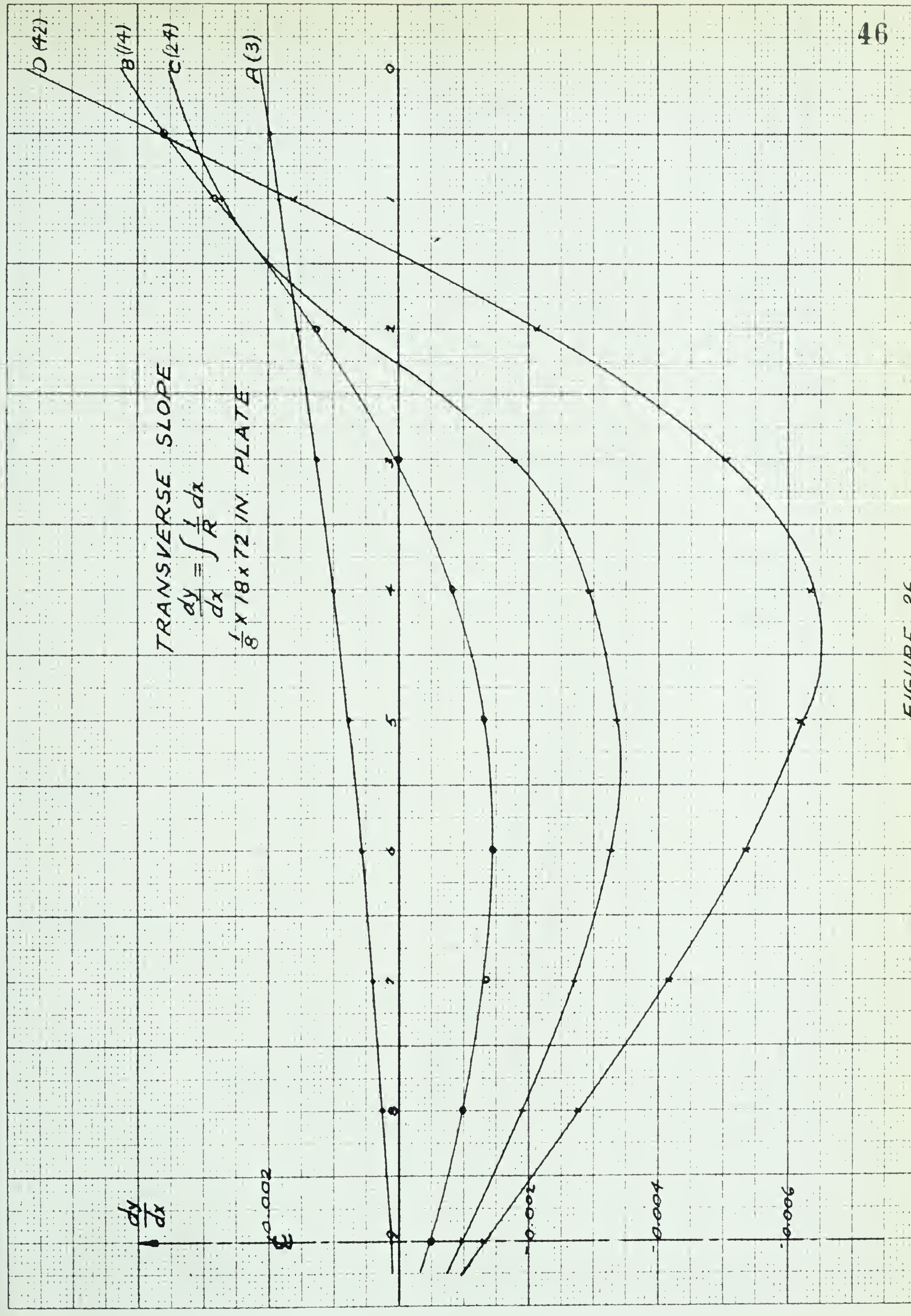

TRANSVERSE SLOPE
$\frac{dy}{dx} = \int \frac{1}{R} dx$
$\frac{1}{8}$ x 18 x 72 IN. PLATE
D (42)
B (14)
C (24)
A (3)
$\frac{dy}{dx}$
0.002
-0.002
-0.004
-0.006
℄
0
1
2
3
4
5
6
7
8
9

FIGURE 26

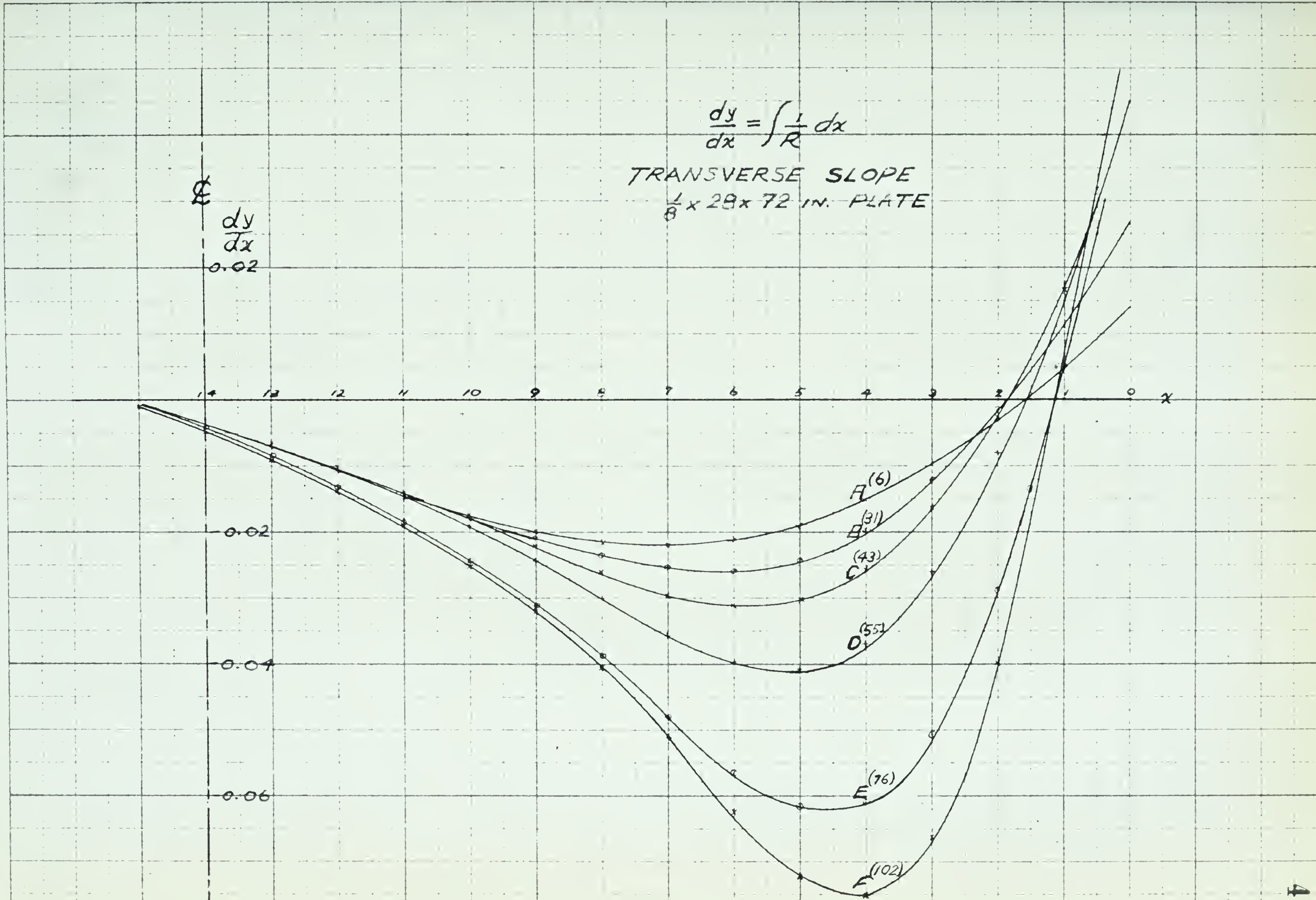

$\frac{dy}{dx} = \int \frac{1}{R} dx$
TRANSVERSE SLOPE
$\frac{1}{8} \times 28 \times 72$ IN. PLATE
℄
$\frac{dy}{dx}$
0.02
0.02
0.04
0.06
14
13
12
11
10
9
8
7
6
5
4
3
2
1
0
x
A(6)
B(31)
C(43)
D(55)
E(76)
F(102)

FIGURE 27

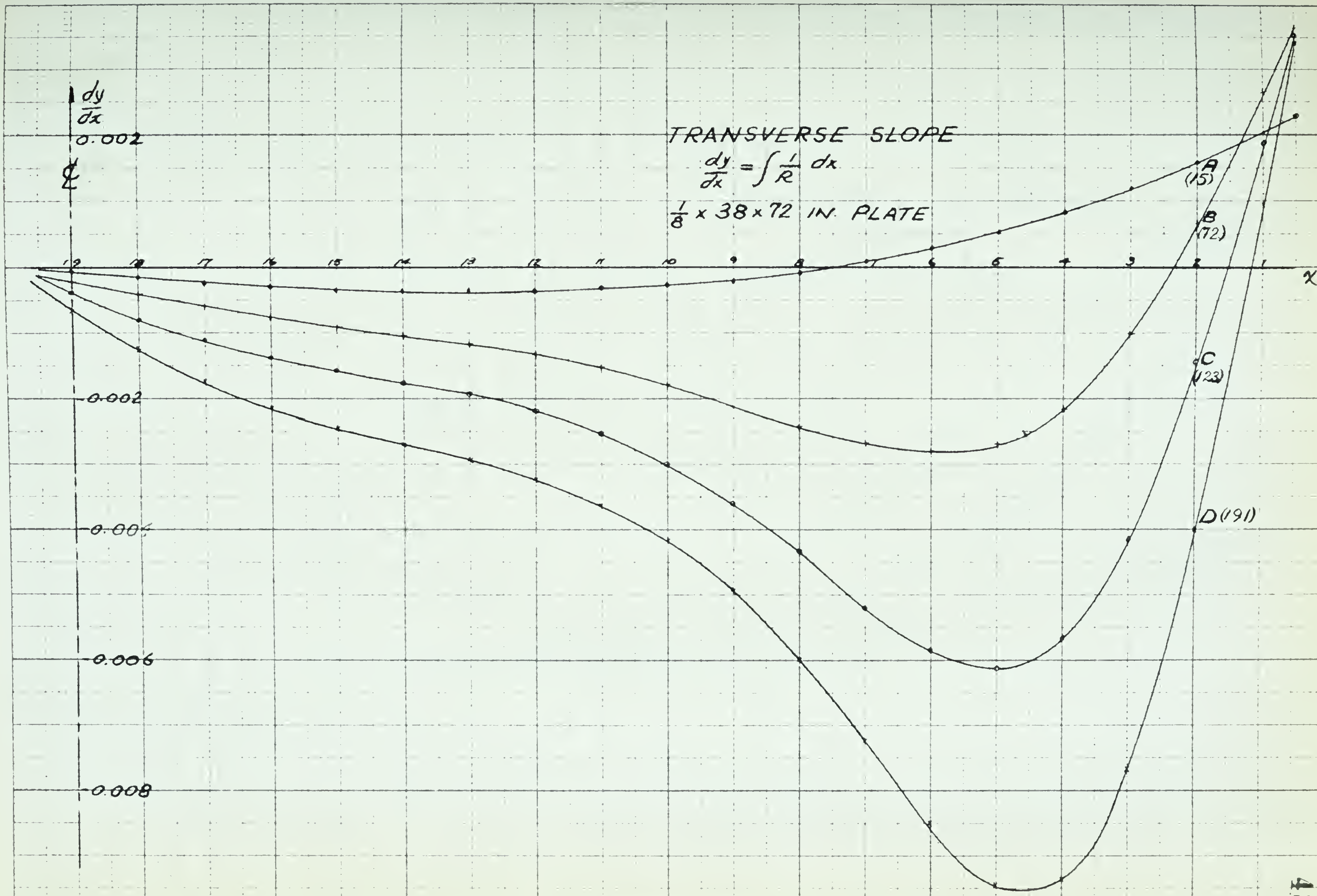

TRANSVERSE SLOPE
$\frac{dy}{dx} = \int \frac{1}{R} dx$
$\frac{7}{8} \times 38 \times 72$ IN. PLATE
$\frac{dy}{dx}$
0.002
0.002
0.004
0.006
0.008
A (15)
B (72)
C (123)
D (191)
x

FIGURE 28

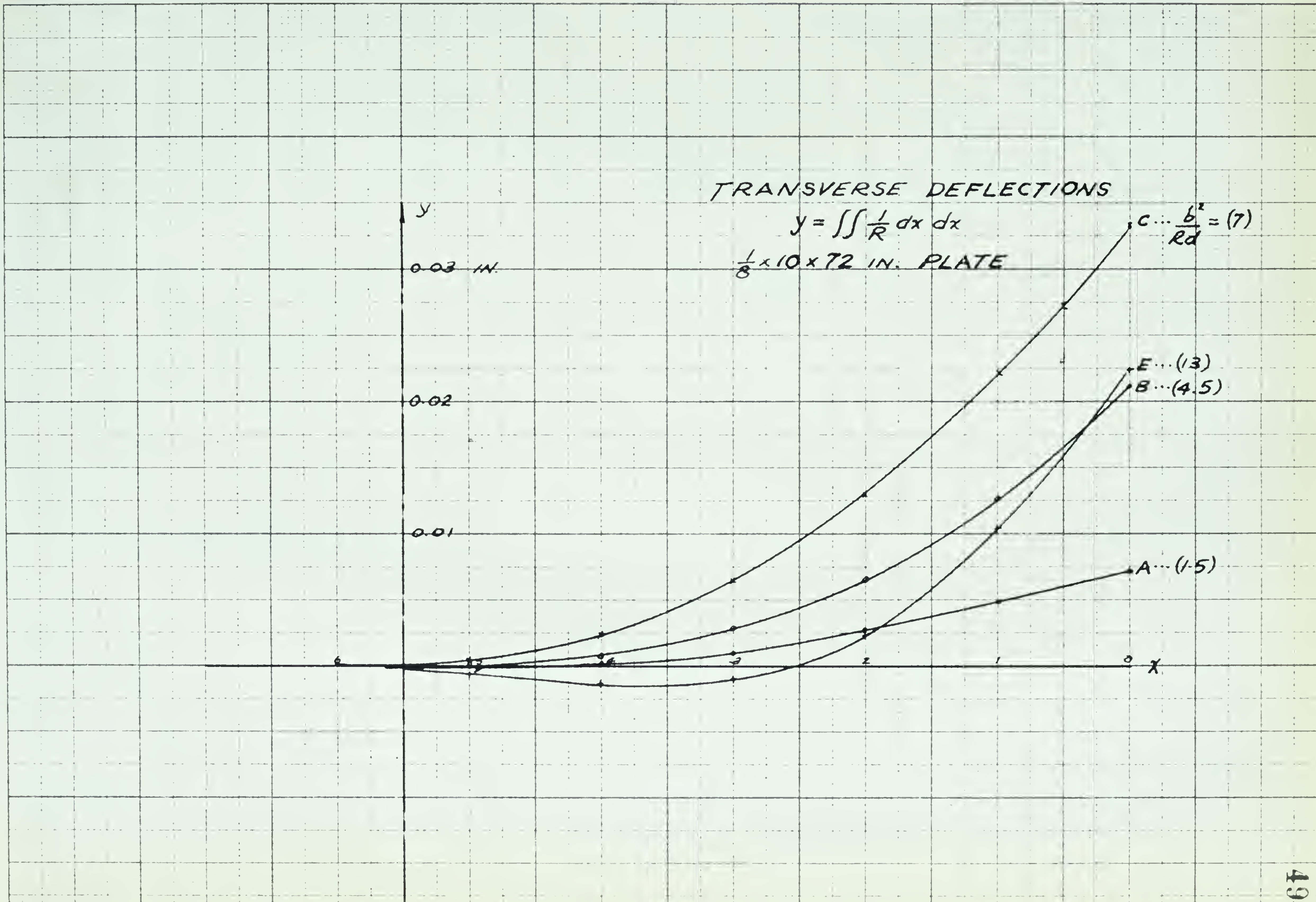
TRANSVERSE DEFLECTIONS
$y = \iint \frac{1}{R}\,dx\,dx$
$\frac{1}{8} \times 10 \times 72$ IN. PLATE
C ... $\frac{b^2}{Rd} = (7)$
E ... (13)
B ... (4.5)
A ... (1.5)
y
0.03 IN.
0.02
0.01
X
0
1
2
3
6

FIGURE 29

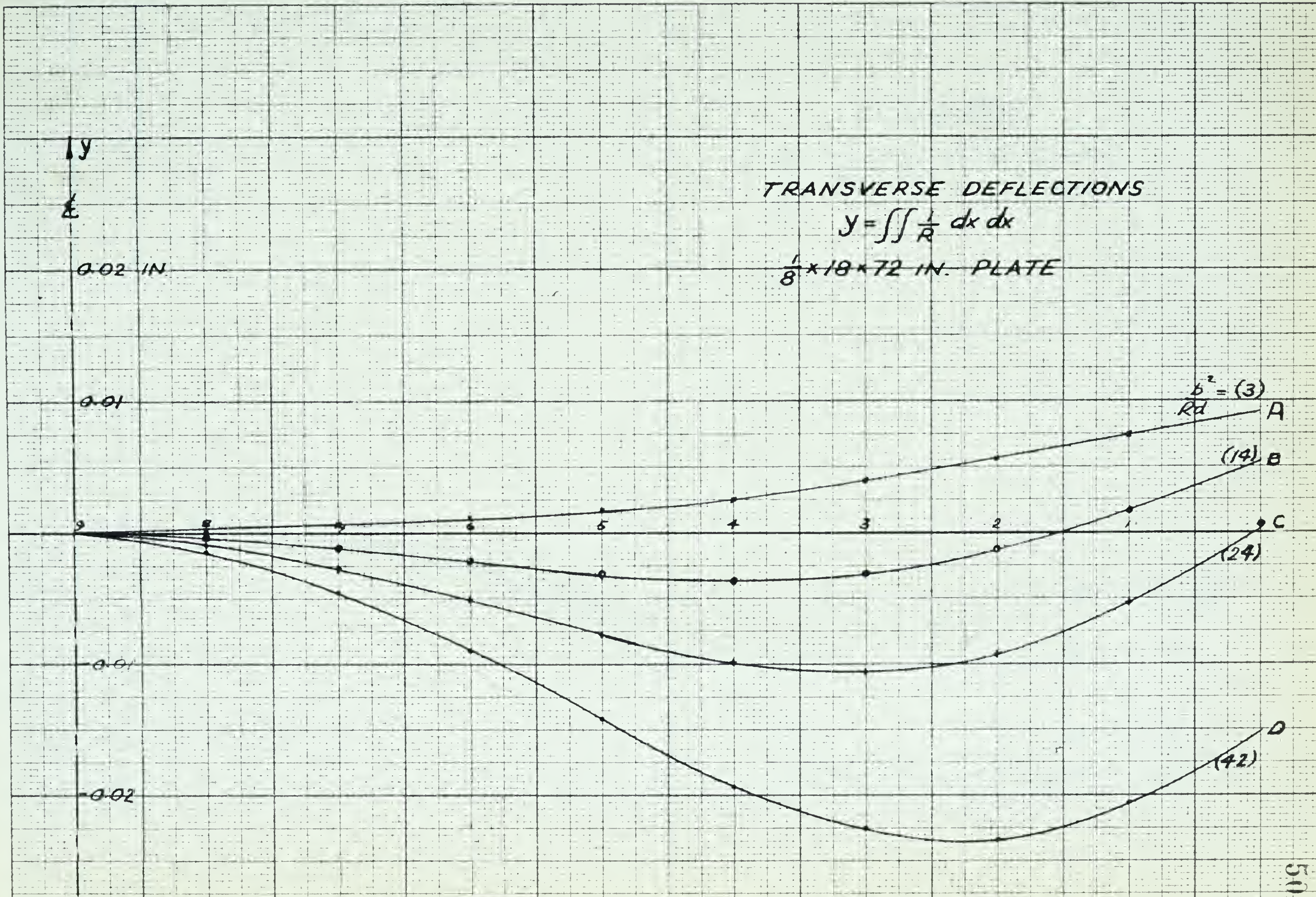

TRANSVERSE DEFLECTIONS
$y = \iint \frac{1}{R}\, dx\, dx$
$\frac{1}{8} \times 18 \times 72$ IN. PLATE
y
℄
0.02 IN
0.01
-0.01
-0.02
9
8
7
6
5
4
3
2
1
$\frac{b^2}{Rd} = (3)$
A
(14)
B
C
(24)
D
(42)

FIGURE 30

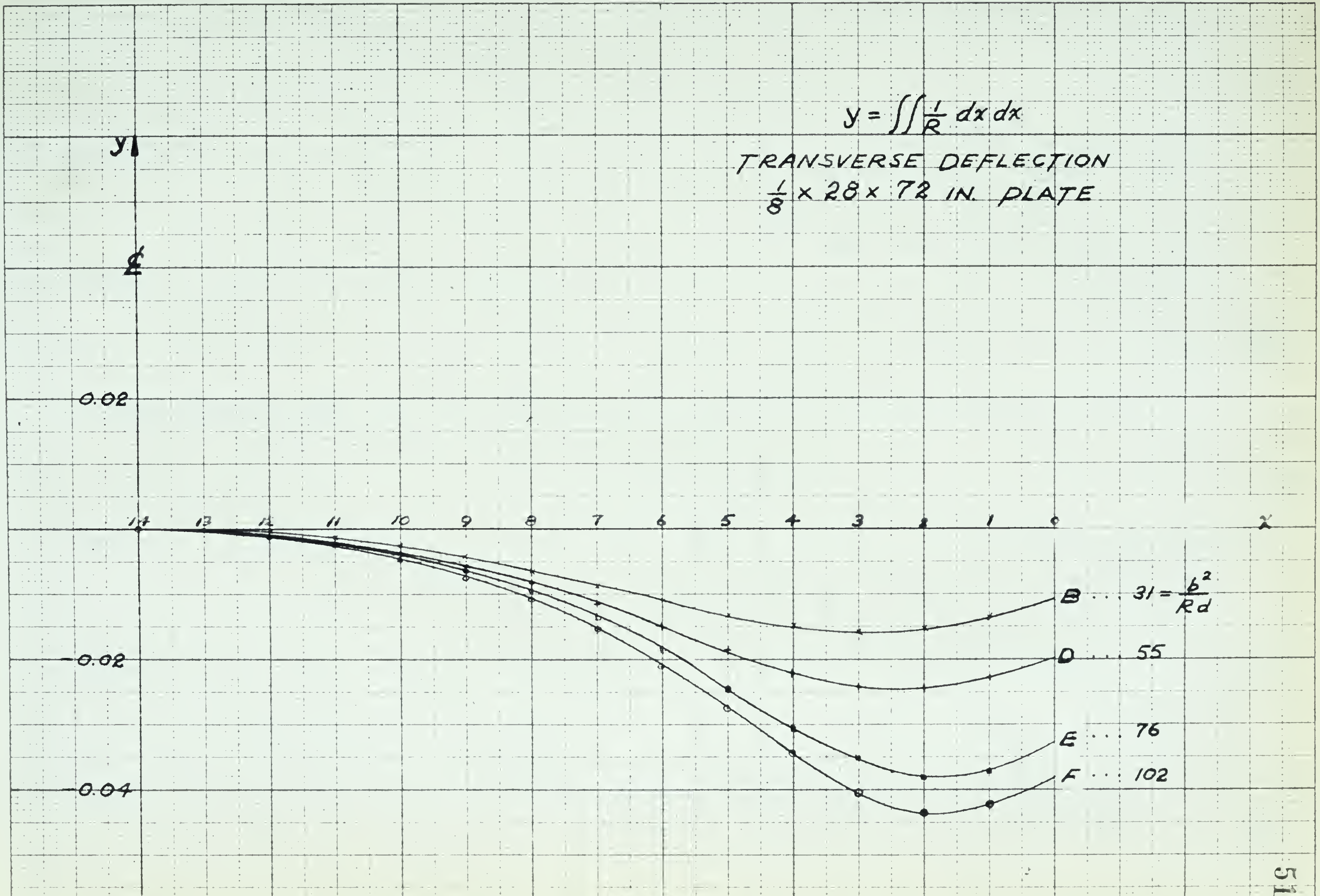
$y = \iint \frac{1}{R}\,dx\,dx$
TRANSVERSE DEFLECTION
$\frac{1}{8} \times 28 \times 72$ IN. PLATE
y
℄
0.02
-0.02
-0.04
14
13
12
11
10
9
8
7
6
5
4
3
2
1
0
x
B . . . $31 = \frac{b^2}{Rd}$
D . . . 55
E . . . 76
F . . . 102

FIGURE 31

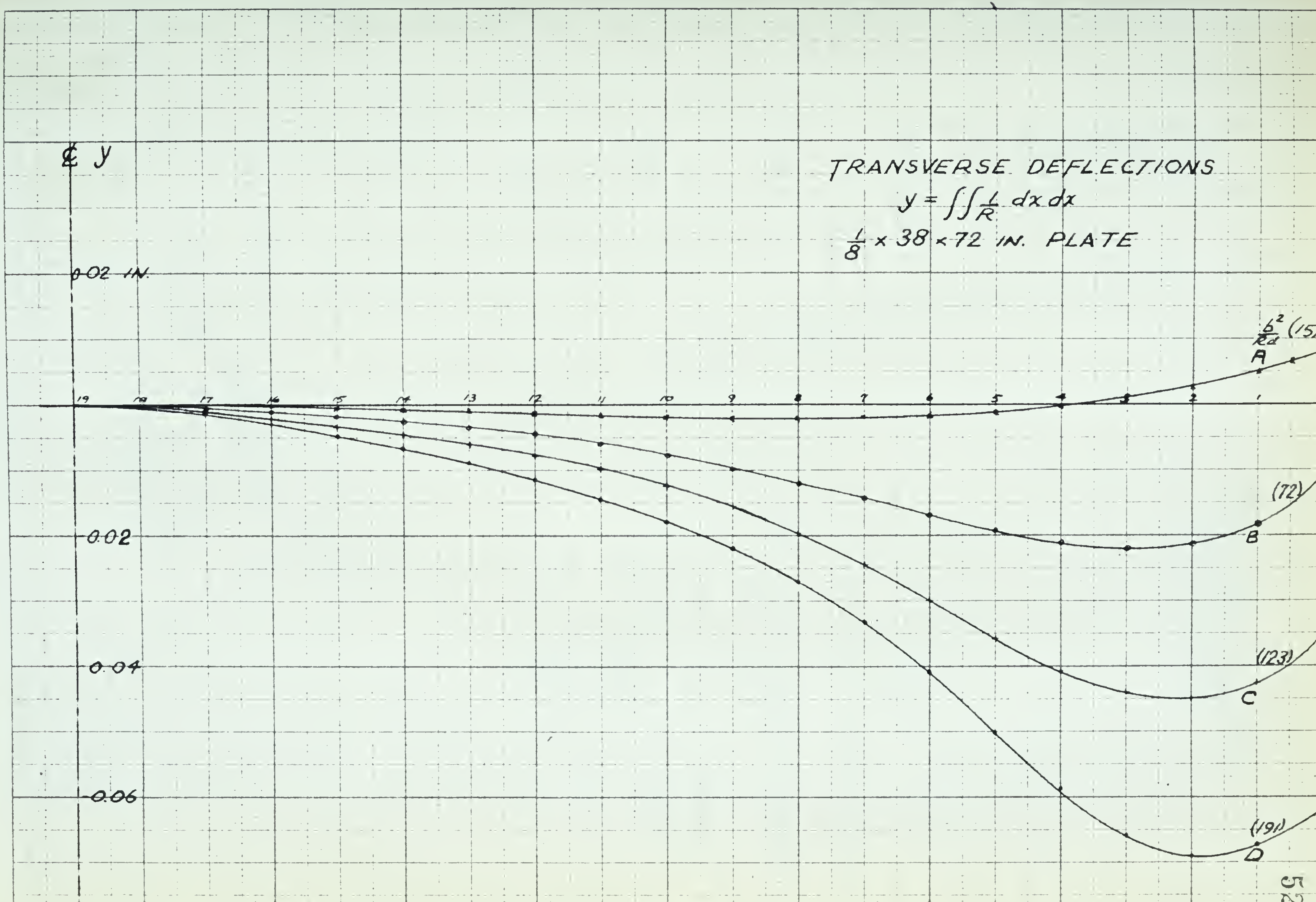
TRANSVERSE DEFLECTIONS
$y = \iint \frac{1}{R}\,dx\,dx$
$\frac{1}{8} \times 38 \times 72$ IN. PLATE
℄ y
0.02 IN.
0.02
0.04
0.06
19 18 17 16 15 14 13 12 11 10 9 8 7 6 5 4 3 2 1 0
A
$\frac{b^2}{Ed}$ (15)
B
(72)
C
(123)
D
(191)

FIGURE 32

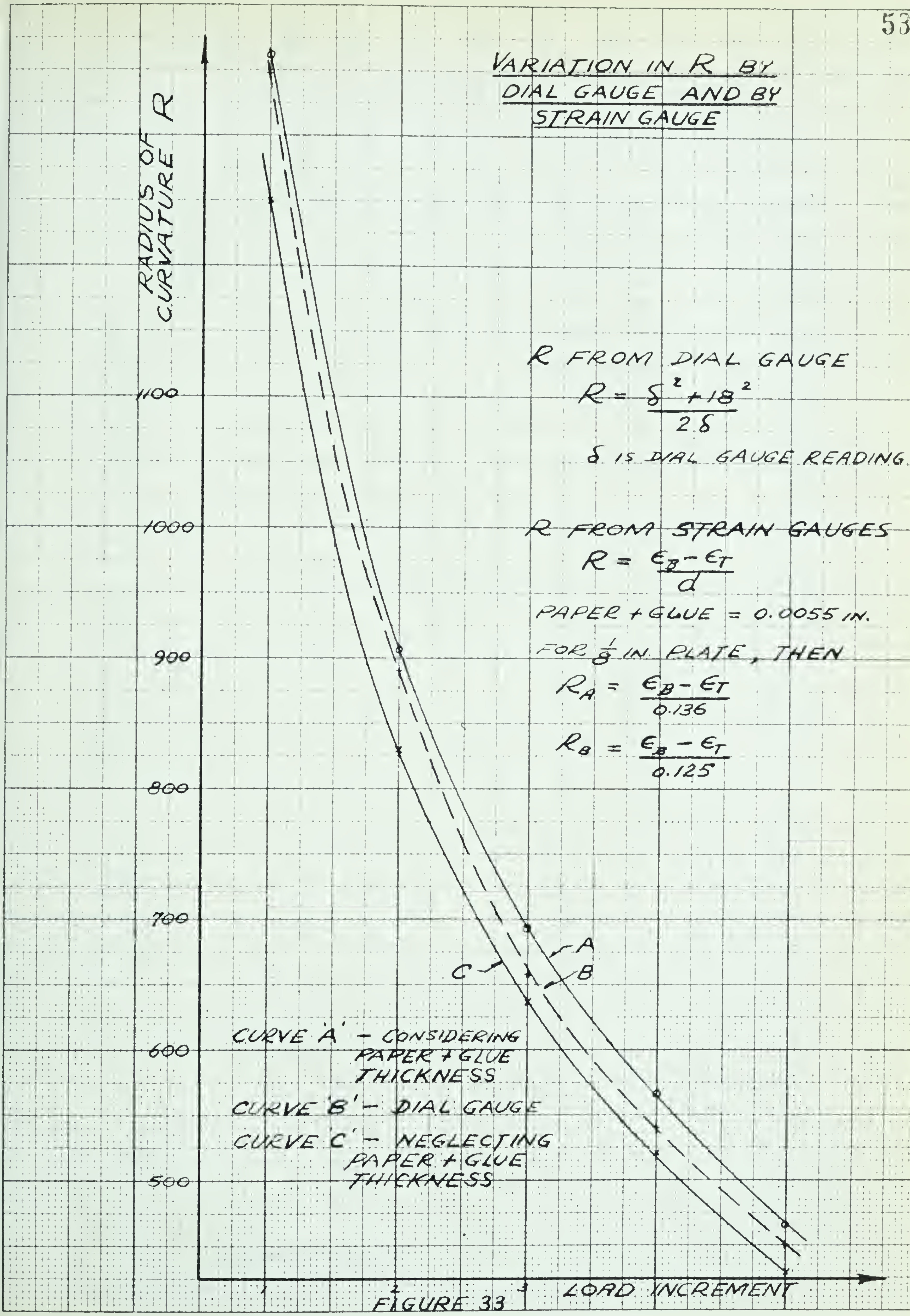
VARIATION IN R BY
DIAL GAUGE AND BY
STRAIN GAUGE
RADIUS OF
CURVATURE R
R FROM DIAL GAUGE
$R = \frac{\delta^2 + 18^2}{2\delta}$
δ IS DIAL GAUGE READING
R FROM STRAIN GAUGES
$R = \frac{\epsilon_B - \epsilon_T}{d}$
PAPER + GLUE = 0.0055 IN.
FOR $\frac{1}{8}$ IN. PLATE, THEN
$R_A = \frac{\epsilon_B - \epsilon_T}{0.136}$
$R_B = \frac{\epsilon_B - \epsilon_T}{0.125}$
1100
1000
900
800
700
600
500
A
B
C
CURVE 'A' - CONSIDERING PAPER + GLUE THICKNESS
CURVE 'B' - DIAL GAUGE
CURVE 'C' - NEGLECTING PAPER + GLUE THICKNESS
1
2
3
LOAD INCREMENT

FIGURE 33

LONGITUDINAL STRAINS FOR $\frac{1}{8} \times 10 \times 72$ IN. PLATE
ILLUSTRATING SAINT-VENANT'S PRINCIPLE

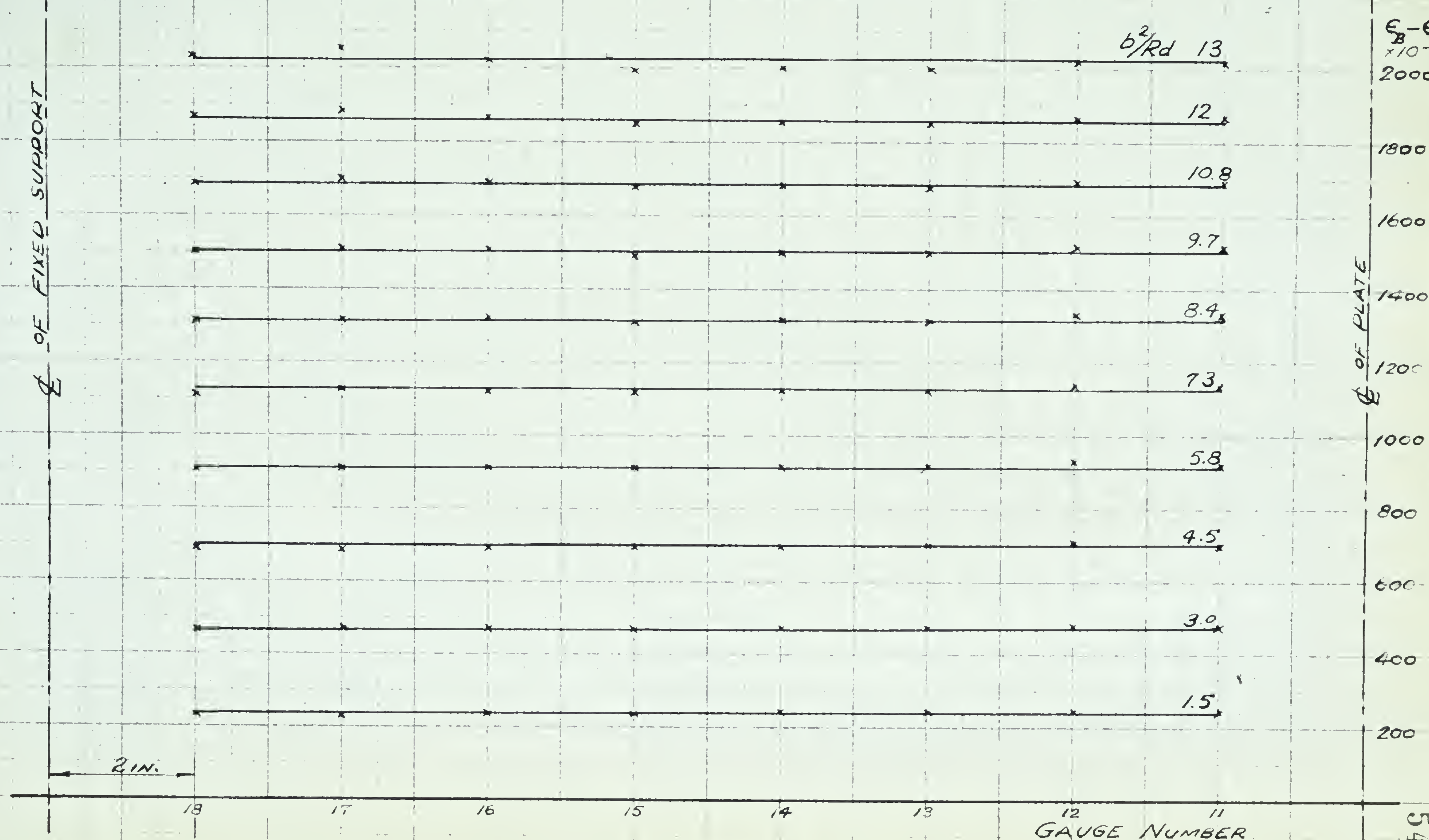

FIGURE 34

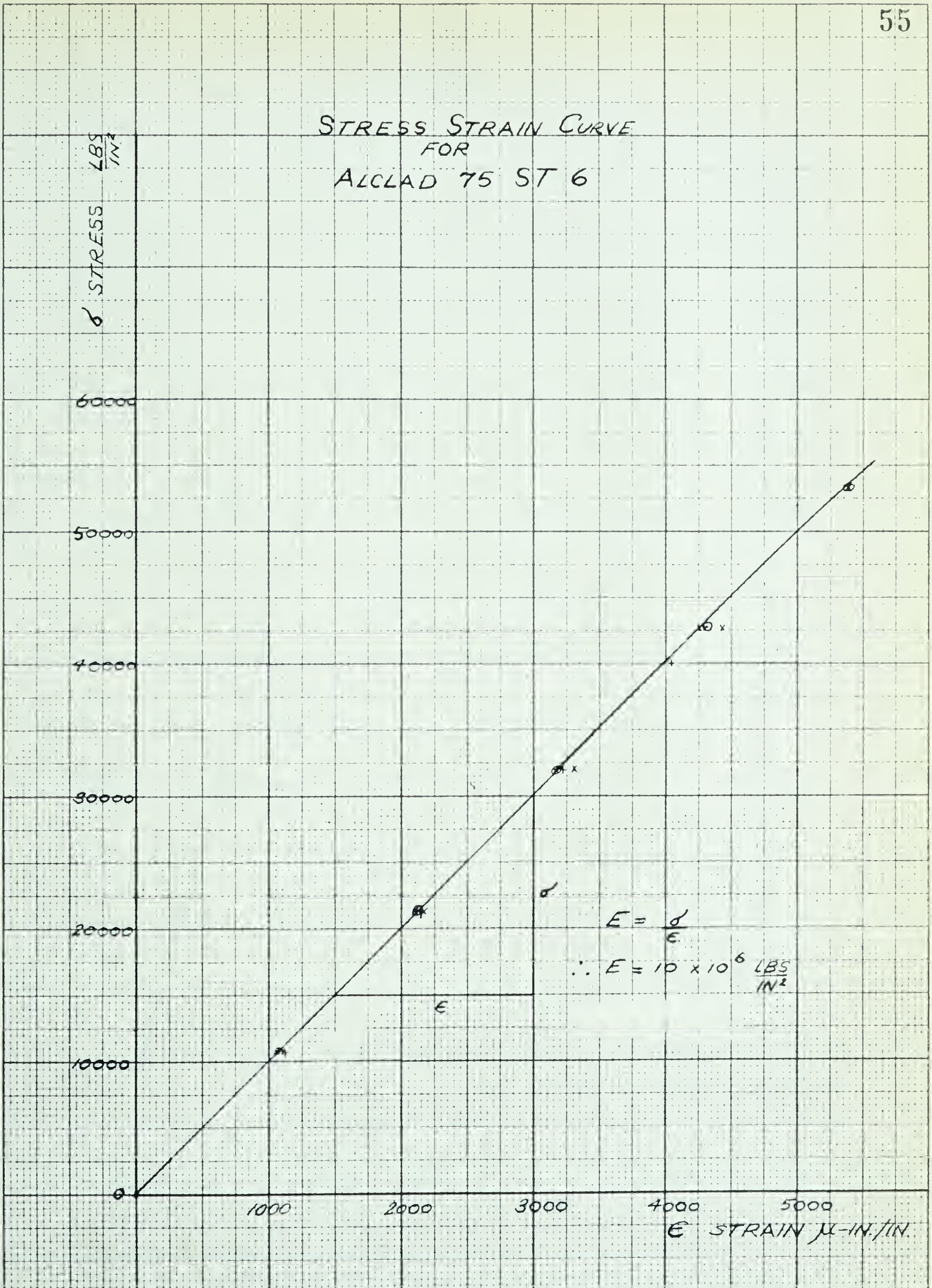
STRESS STRAIN CURVE
FOR
ALCLAD 75 ST 6
σ STRESS LBS/IN²
60000
50000
40000
30000
20000
10000
0
1000
2000
3000
4000
5000
ϵ STRAIN μ-IN./IN.
σ
ϵ
E = σ/ϵ
∴ E = 10 x 10⁶ LBS/IN²

FIGURE 35

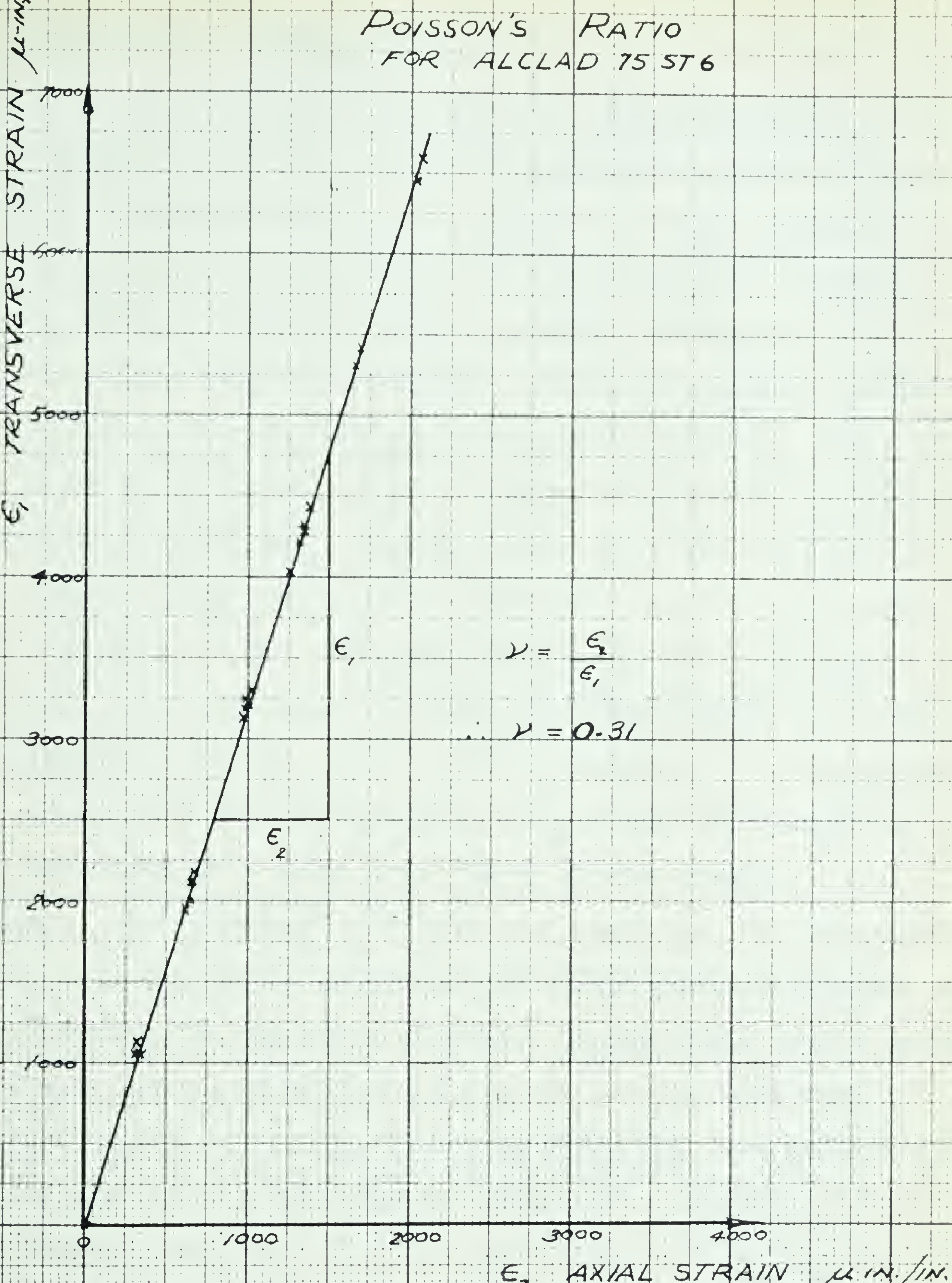
POISSON'S RATIO
FOR ALCLAD 75 ST 6
ϵ_1 TRANSVERSE STRAIN μ-IN/IN.
7000
6000
5000
4000
3000
2000
1000
0
1000
2000
3000
4000
ϵ_2 AXIAL STRAIN μ IN./IN.
ϵ_1
ϵ_2
$\nu = \frac{\epsilon_2}{\epsilon_1}$
$\therefore \nu = 0.31$

FIGURE 36

Chapter 5 - CONCLUSIONS

1. It was found that the value $\frac{b^2}{Rd}$ represented a true physical ratio and that its magnitude described the mode of transverse bending. For $\frac{b^2}{Rd} < 16$ the transverse curvature was anticlastic, while, for $\frac{b^2}{Rd} > 22$ the transverse curvature was essentially synclastic. It is concluded that the transverse curvature changes from an anticlastic to a synclastic mode when $16 < \frac{b^2}{Rd} < 22$. This is a contradiction to what has been written by Ashwell and Fung and Wittrick. However, even under the influence of $\frac{b^2}{Rd} = 191$, there was no indication of the radius of curvature in the transverse direction being infinite.

2. For the range of strain readings observed and plate thickness tested, it was found permissable to neglect the paper plus glue thickness in calculating the radius of curvature at a point from "SR-4" strain gauges.

3. Saint-Venant's Principle was observed in this thesis by placing strain gauges in the longitudinal direction, every 2 inches, on the plate surface. It was found that 2 inches away from the disturbing force the strains were uniform and unaffected by the manner in which the load was applied, thereby, justifying the size of plates, and method of loading, chosen.

4. The mechanical properties for each plate tested were identical and thus $\frac{b^2}{Rd}$ values for each plate size were observed and compared without being influenced by the material properties.

5. It was, therefore, concluded that strain gauges provide a good method of observing the shape and transformation of the transverse curvature, slope, and deflection.

6. The ratio $\frac{b2}{Rd}$ is a very important parameter in the use of the equation $M = \frac{EI}{\phi R}$. The value ϕ must have is clearly depended on the $\frac{b^2}{Rd}$ value. Two known conditions for ϕ exist; that is, $\phi = 1$ for a beam whose $\frac{b^2}{Rd} \ll 12$ or more precise, for $\frac{b^2}{Rd} < 1$, and the case for an infinitely wide plate, $\phi = \frac{1}{(1-\nu^2)}$.

Chapter 6 - RECOMMENDATIONS

1. The work of this thesis was carried out with a view of testing plates at large $\frac{b^2}{Rd}$ values. It would be desirable to experiment around low $\frac{b^2}{Rd}$ values and observe a transition point or points which may occur when the transverse strip changes from beam action to plate action. This could be done with the existing plates and apparatus. However, for low $\frac{b^2}{Rd}$ values the strains are small and hence, the experimental results will be greatly influenced by the accuracy of the measuring instruments. It would be desirable to devise a means which could amplify the strains recorded and hence, increase the experimental accuracy. It should be noted that the strain indicator used for this work was capable of measuring to the nearest 5×10^{-6} inch/inch.

2. This was an experimental thesis. It would be desirable, in the light of the experimental evidence, to compare these results with the theoretical; especially compare to a plate with an initial transverse curvature. This would determine whether or not the initial curvature has such a great effect on the final curvature as indicated by Ashwell.

3. It would be interesting to further investigate Saint-Venant's Principle. It is believed that strain gauges offer a very useful tool in observing this principle.

4. Because the strain values obtained in this experiment are much lower than the yield strain for aluminum it is difficult to see how any initial residual strains could have been incurred. If this is true then the discrepancy in the experimental curves and Ashwell's theoretical calculations must be due to some other factor or factors. It is suggested that the discrepancy may lie in the boundary conditions chosen by Ashwell to evaluate the solution of the fourth order differential equation on Page 9 (Equation 3). The general solution to this equation is;

$$y = \exp \frac{kx}{\sqrt{2}} \left(A \cos \frac{kx}{\sqrt{2}} + B \sin \frac{kx}{\sqrt{2}}\right) + \exp \frac{-kx}{\sqrt{2}} \left(C \cos \frac{kx}{\sqrt{2}} + D \sin \frac{kx}{\sqrt{2}}\right)$$

where $$K^4 = \frac{(12)\,(1 - \nu^2)}{d^2 R^2}$$

To evaluate the constants A, B, C, D, Ashwell assumed the following;

1. At $x = \pm \frac{b}{2}$ $\quad \frac{d^3 y}{dx^3} = 0$

2. At $x = \pm \frac{b}{2}$ $\quad \frac{d^2 y}{dx^2} = \frac{\nu}{R}$

3. Because of symmetry, y is an even function of x.

If the plate equation 3 is correct, and the experimental curves are correct, then the only possible reason for the discrepancy between experiment and theory must be that the above boundary conditions are wrong. Therefore, it is recommended that the above general solution be made to fit the experimental curves and thus, determine the true boundary conditions.

Chapter 7 - BIBLIOGRAPHY

1. G.F.C. Searle, Experimental Elasticity Cambridge 1908, pp. 40-58.

2. J. Case, Strength of Materials, third edition, Arnold 1938, pp. 546-554.

3. D.G. Ashwell, "The Anticlastic Curvature of Rectangular Beams and Plates", Journal of Royal Aeronautical Society, Vo. 45, 1950, p. 708.

4. Y.C. Fung, W.H. Wittrick, "A Boundary Layer Phenomenon in the Large Deflexion of Thin Plates", Quarterly Journal of Mechanics and Applied Mathematics, Vol. VIII, Part 2, 1955.

5. D.G. Ashwell, E.D. Greenwood, "The Pure Bending of Rectangular Plates", Engineering, 21 and 28 July, 1950.

6. A.H. Hall, H.F.L. Pinkney, Hellen Tullock, "On the Analytical Determination of the Normal Modes and Frequencies of Swept Cantilever Vibrations", National Aeronautical Establishment Canada, Report 21, 1953.

7. A.H. Hall, Private Communication to G. Ford, June 16, 1959.

8. D.G. Ashwell, E.D. Greenwood, "Measuring Small Changes in Curvature with an Angle Dekkor", Machinery, Dec. 16, 1948.

9. J.P. Den Hartog, Advanced Strength of Materials, McGraw-Hill, 1952, p. 184.

10. A.E.H. Love, A Treatise on the Mathematical Theory of Elasticity, Dover 1944, p. 556.

APPENDIX A

Theory of Searle and Case

Case and Searle said when a beam is longitudinally bent to a radius R, there develop radially forces which tend to neutralize the anticlastic curvature. Their argument is as follows;

For a beam width b, depth d, and bent to a radius R (see Figure 3). The resultant downward force acting on an element, if above neutral axis (upward resultant if below neutral axis) is,

$$= \sigma \, dA \, \frac{d\theta}{2} \cdot 2$$

$$\text{but} \quad dS = R d\theta$$

$$\text{therefore, resultant} = \sigma \, dA \, \frac{dS}{R}$$

$$= \frac{yE}{R^2} \, dA \, dS$$

Considering the transverse section of this beam, it is known that it is bent to a radius of curvature $\frac{R}{\nu}$ which is anticlastic to the longitudinal curvature. Figure 37 shows that the element ab will be pulled radially inwards towards the x-axis while element bc will be pushed radially outwards from the x-axis.

Thus, if $ab > bc$ resultant will be an inward "pull"

if $bc > ab$ resultant will be an outward "push"

Now ab will be pulled inward with a force equal to

$$\int_b^a \frac{yE}{R^2}\, dA\, dS$$

On element ac the net resultant will be a radial upward "push". On element a'c' the resultant will be a radial downward pull. Thus, each side of the transverse element is subjected to a couple as shown in Figure 37. The effect of these couples is to reduce the anticlastic curvature.

To reduce the anticlastic curvature the couples on the transverse beam will have to be significant. The effectiveness of these couples will depend on the height $\overline{O}H$. H is the centroid of the section. If $\overline{O}H$ is small compared to $\frac{d}{2}$ then these couples will have little effect on the transverse curvature. Such is the known case of a beam where the curvature is $\frac{\nu}{R}$.

Therefore,

$$\left(\frac{R}{\nu} - \overline{O}H\right)^2 + \left(\frac{b}{2}\right)^2 = \left(\frac{R}{\nu}\right)^2$$

$$-\frac{2R}{\nu} \cdot \overline{O}H + \overline{O}H^2 + \frac{b^2}{4} = 0$$

if $\overline{O}H$ is small then $(\overline{O}H)^2$ is negligible

therefore, $\overline{O}H = \frac{b^2 \nu}{8R}$

but $\overline{O}H$ is small for a beam

i.e., $\overline{O}H << \frac{d}{2}$

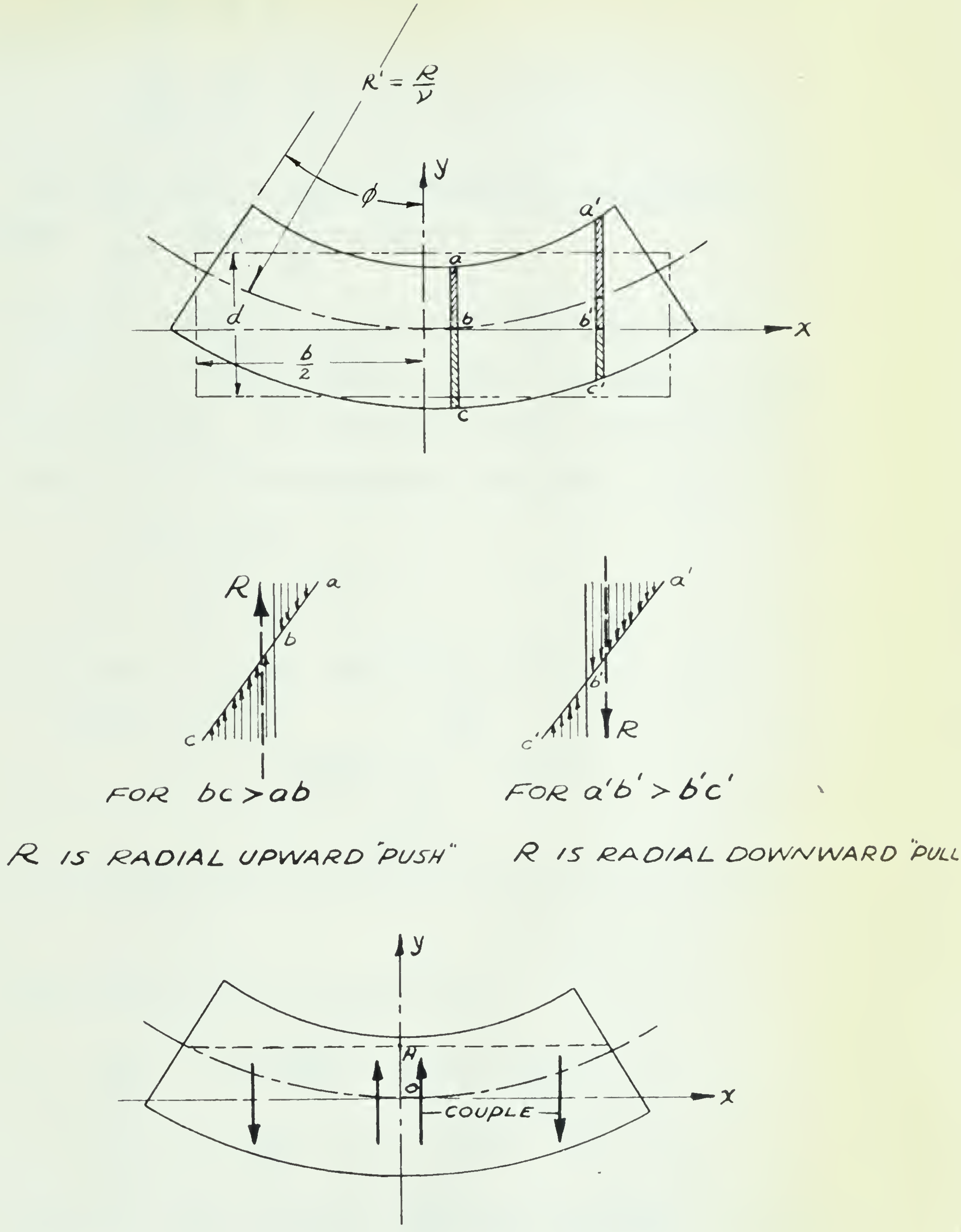

FIGURE 37 FORCES ON A BEAM

$$\text{or,}\quad \frac{b^2\nu}{8R} << \frac{d}{2}$$

$$\frac{b^2}{Rd} << 12 \qquad \text{for} \qquad \nu = 1/3$$

This says, for a beam to retain its anticlastic curvature $\frac{\nu}{R}$ then $\frac{b^2}{Rd} << 12.$

The above analysis is not sufficient for a plate because the height $\overline{OH}$ no longer is small compared to half the plate thickness. The resultant radial force acting on an element dx in the transverse direction is equal to,

$$\sigma\, d.\ d\theta\ dx$$

$$\text{or,}\ = \frac{yE}{R}\, d.\ d\theta.\ dx$$

The moment of this force about the y-axis is M'.

where

$$M' = \frac{Ed.d\theta}{R}\int_0^{\frac{b}{2}} x\ y\ dx$$

To integrate this equation it is required to relate x and y.

From Figure 3 it is known that

$$\left[\frac{R}{\nu} - (y + \overline{OC})\right]^2 + x^2 = \left(\frac{R}{\nu}\right)^2$$

$$-\frac{2R}{\nu}(y + \overline{OC}) + (y + \overline{OC})^2 + x^2 = 0$$

but $(y + \overline{OC})$ is small, therefore $(y + \overline{OC})^2 \doteq 0$

$$\text{or,}\quad y = \frac{\nu x^2}{2R} - \overline{OC}$$

But, the centroid of the arc about the center of curvature is $\bar{y} = \frac{R}{\nu} \frac{\sin \phi}{\phi}$

$$\text{therefore,} \quad \overline{OC} = \frac{R}{\nu} \left(1 - \frac{\sin \phi}{\phi}\right)$$

where $\overline{OC}$ is the distance from the centroid to the middle fibre.

Now,

$$\frac{\sin \phi}{\phi} = \frac{1}{\phi}\left(\phi - \frac{\phi^3}{3!} + \ldots\right) = 1 - \frac{\phi^3}{3!} + \ldots$$

$$\text{therefore,} \quad \overline{OC} \doteq \frac{R}{\nu} \frac{\phi^2}{6}$$

$$\text{hence,} \quad y = \frac{x^2}{2R} - \frac{R}{\nu} \frac{\phi^2}{6}$$

$$= \frac{x^2}{2R'} - \frac{R'\phi^2}{6}$$

$$\text{but,} \quad \phi = \frac{\frac{b}{2}}{R'}$$

$$\phi^2 = \frac{b^2}{4(R')^2}$$

$$\text{therefore,} \quad y = \frac{x^2}{2R'} - \frac{b^2}{24R'}$$

Moment becomes,

$$M' = \frac{Ed.d\theta}{R} \int_0^{\frac{b}{2}} \left(\frac{x^3}{2R'} - \frac{b^2 x}{24R'}\right) dx$$

$$M' = \frac{Ed.d\theta}{RR'} \left(\frac{b^4}{4x2x16} - \frac{b^4}{24x2x4}\right)$$

hence, $$M' = \frac{Ed.d\theta\, b^4}{384\, RR'}$$

The effect of the bending moment M' is to reduce the anticlastic curvature. To find this effect consider an element in the transverse direction as before.

For the element $$I = \frac{Rd\theta\, d^3}{12}$$

Now if the transverse curvature is to be neutralized by the moment M' and $\frac{1}{\rho}$ is the change in curvature caused by M' then

$$\frac{1}{\rho} = \frac{M'}{EI} = \frac{Ed.\,d\phi\, b^4}{384\, RR'\, E} \cdot \frac{12}{Rd\phi\, d^3}$$

or, $$\frac{1}{\rho} = \frac{b^4}{32\, R^2 R'\, d^2}$$

$\frac{1}{\rho}$ represents a decrease in curvature. Thus, anticlastic curvature will be neutralized when $\frac{1}{\rho} > \frac{1}{R'}$

or, from the above,

$$\frac{1}{\rho} > \frac{1}{R'} \quad \text{if} \quad b^4 > 32\, R^2 d^2$$

i.e., $$\frac{b^2}{Rd} > \sqrt{32} \doteq 6$$

Thus, for $\frac{b^2}{Rd} > 6$ the anticlastic curvature will be neutralized. This is the result expressed by Searle and Case.

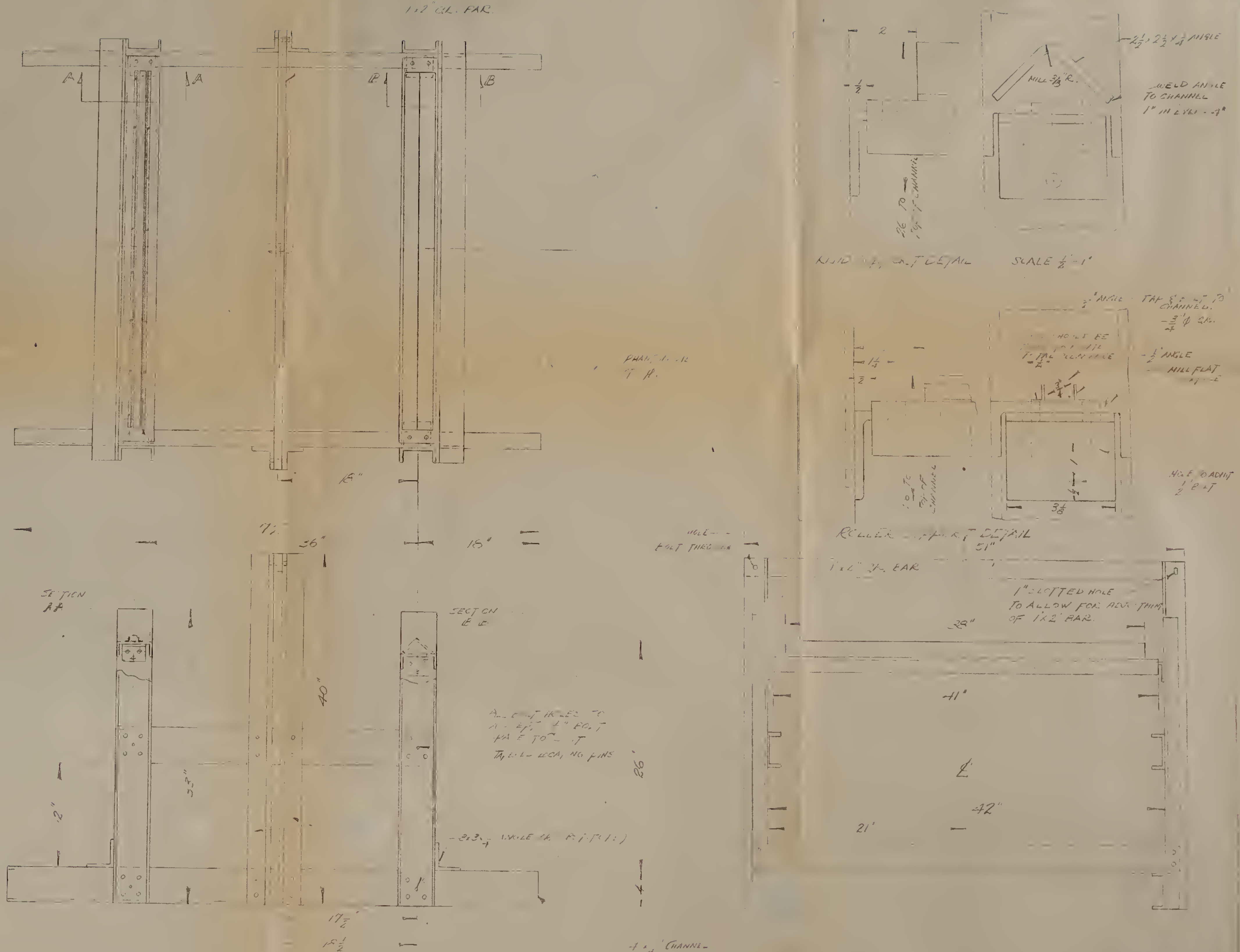

- 3/4" ROLLER IS TO REMAIN FREE
ALL BOLTS TO GO COMPLETELY THROUGH WITH LOCK WASHER AND NUT ON OTHER SIDE.
— NOTE THAT THE HEIGHT OF THE [illegible] OF THE ROLLER AND THE HEIGHT [illegible] ANGLE IS 26" [illegible] CHANNEL ON FLOOR.

TEST FIXTURE
DEPT OF APPLIED MECHANICS
UNIVERSITY OF ALBERTA

SCALE [illegible] UNLESS NOTED OTHERWISE

NOV [illegible] D. G. B[illegible]

APPENDIX B

- APPENDIX C

Method of Integrating Strain Curves

The slope α , at any point, is given by the rate of change of deflection.

i.e., $$\alpha = \frac{dy}{dx} \quad \ldots\ldots\ldots\ldots\ldots\ldots\ldots \quad 1$$

Also, $R\,d\alpha = ds$

or, $$\frac{1}{R} = \frac{d\alpha}{ds} \quad \ldots\ldots\ldots\ldots\ldots\ldots\ldots \quad 2$$

For small angle changes it can be assumed that $dx \doteq ds$ then equation 2 becomes,

$$\frac{1}{R} = \frac{d\alpha}{dx} \quad \ldots\ldots\ldots\ldots\ldots\ldots\ldots \quad 2a$$

From 1 and 2a

$$\frac{1}{R} = \frac{d\alpha}{dx} \doteq \frac{d^2y}{dx^2}$$

therefore, $$\frac{1}{R} \doteq \frac{d^2y}{dx^2} \quad \ldots\ldots\ldots\ldots\ldots\ldots\ldots \quad 3$$

Equation 3 is valid if the slope is small. Experimental work in this thesis showed that $\frac{dy}{dx} = 0\ (0.009)$. Hence, the approximation is justified.

By integrating equation 3 once, the slope was obtained, and by integrating a second time the deflection was obtained.

i.e.,

$$\frac{1}{R} = \frac{d^2y}{dx^2} \quad \ldots\ldots\ldots\ldots\ldots\ldots\ldots\ 3$$

$$\frac{dy}{dx} = \int \frac{1}{R}\, dx \quad \ldots\ldots\ldots\ldots\ldots\ldots\ 4$$

$$y = \iint \frac{1}{R}\, dx\, dx \quad \ldots\ldots\ldots\ldots\ldots\ 5$$

Strains were measured on the top and bottom of the plate. Plotting the bottom strain minus the top strain $e_B - e_T$ versus the transverse distance x yielded a curve which was proportional to the curvature.

$$\text{since,} \quad e = \frac{y}{R}$$

$$\text{then,} \quad \frac{1}{R} = \frac{e_B - e_T}{d} \quad \ldots\ldots\ 6$$

$e_B - e_T$ was know for each point across the width of the plate. Therefore, by integrating the transverse strain curve with respect to x the slope curve was obtained. Integrating the slope curve with respect to x yielded the deflection curve.